Arabian Journal of Chemistry (2012) 5, 1–23

King Saud University

Arabian Journal of Chemistry

www.ksu.edu.sa
www.sciencedirect.com

REVIEW

Carbon nanotubes, science and technology part (I) structure, synthesis and characterisation

Ahmad Aqel [a,*], **Kholoud M.M. Abou El-Nour** [b], **Reda A.A. Ammar** [c], **Abdulrahman Al-Warthan** [c]

[a] *King Abdullah Institute for Nanotechnology, College of Science building # 4, P.O. Box 2454, King Saud University, Riyadh 11451, Saudi Arabia*
[b] *Department of Chemistry, College of Science, King Faisal University, Hufof-31982, P.O. Box 4710, Al-Ahsa, Saudi Arabia*
[c] *Department of Chemistry, College of Science building # 5, P.O. Box 2455, King Saud University, Riyadh 11451, Saudi Arabia*

Received 9 June 2010; accepted 28 August 2010
Available online 7 September 2010

KEYWORDS

Nanotechnology;
Carbon nanotubes;
Fullerenes;
Single-wall carbon nanotubes;
Multi-wall carbon nanotubes;
Structure;
Arc discharge;
Chemical vapour deposition;
Laser ablation;
Characterisation methods

Abstract Since their discovery in 1991 by the Japanese scientist "Sumio Iijima", carbon nanotubes have been of great interest, both from a fundamental point of view and for future applications. Different types of carbon nanotubes can be produced in various ways. Economically feasible large-scale production and purification techniques are still under development. Carbon nanotubes are discussed in this review in terms of history, types, structure, synthesis and characterisation methods. Carbon nanotubes have attracted the fancy of many scientists worldwide. The unique and unusual properties of these structures make them a unique material with a whole range of promising applications.

© 2010 King Saud University. Production and hosting by Elsevier B.V. All rights reserved.

---

[*] Corresponding author. Tel.: +96614674198; fax: +96614670662; Mobile: +966505284007.
E-mail addresses: ahmad3qel@yahoo.com, aifseisi@ksu.edu.sa (A. Aqel).

1878-5352 © 2010 King Saud University. Production and hosting by Elsevier B.V. All rights reserved.

Peer review under responsibility of King Saud University.
doi:10.1016/j.arabjc.2010.08.022

ELSEVIER
Production and hosting by Elsevier

Contents

1. Introduction . . . 2
2. History of CNTs . . . 3
3. Types of CNTs . . . 4
    3.1. Single-walled . . . 4
    3.2. Multi-walled . . . 6
4. Structure of CNTs . . . 7
5. Synthesis of CNTs . . . 8
6. Purification of CNTs . . . 9
    6.1. Oxidation . . . 11
    6.2. Acid treatment . . . 11
    6.3. Annealing and thermal treatment . . . 12
    6.4. Ultrasonication . . . 12
    6.5. Magnetic purification . . . 12
    6.6. Micro-filtration . . . 12
    6.7. Cutting . . . 13
    6.8. Functionalisation . . . 13
    6.9. Chromatography . . . 13
7. Characterisation of CNTs . . . 13
    7.1. Photoluminescence spectroscopy . . . 13
    7.2. X-ray photoelectron spectroscopy (XPS) . . . 14
    7.3. Electron microscopy (SEM & TEM) . . . 14
    7.4. Scanning tunneling microscopy (STM) . . . 15
    7.5. X-ray diffraction (XRD) . . . 15
    7.6. Neutron diffraction . . . 17
    7.7. Raman spectroscopy . . . 17
    7.8. Thermal analysis (TGA/DTG) . . . 18
    7.9. Absorption spectroscopy (UV, Vis and IR) . . . 18
8. Conclusion . . . 20
References . . . 20

1. Introduction

Nanoscience is the study, understanding and control of phenomena and manipulation of material at the nanoscale, so nanoscience is the world of atoms, molecules, macromolecules, quantum dots, and macromolecular assemblies. Research in nanoscience is an interdisciplinary knowledge which means that it is a whole knowledge on fundamental properties of nano-sized objects but not limited to physics, chemistry, biology, medicine, engineering, and materials science. Nanotechnology describes many diverse technologies and tools, which do not always appear to have much in common! Therefore, it is better to talk about nanotechnologies, in the plural (Roco, 1999; Dolmer, 2003).

In recent years, miniaturised products have become increasingly dominant in every aspect of life. The benefits of having smaller components, and hence a device with enhanced capabilities and functionalities, are obvious from the following perspectives: smaller systems tend to move more quickly than larger systems because of lower inertia of mass, the minute sizes of small devices encounter fewer problems in thermal distortion and vibration, and they consume less power and then cost (Hsu, 2002). Because of these advantages, miniaturisation of systems and devices has become an active area of research. More broadly, nanotechnology includes the many structures and techniques at a size scale below 100 nm, including carbon nanotubes, nanocrystals, quantum dots, nanofibers, nonoporous filters, nanowires, nanoparticulate metal oxides, nanopillar, dispersion nanoparticles, nanopin film, polymer nanocomposites, and others…

As is the case with numerous important scientific discoveries, fullerenes were accidentally discovered. In 1985, scientists discovered new material by founding strange results in mass spectra of evaporated carbon samples (Kroto et al., 1985). Herewith, fullerenes were discovered and their stability in the gas phase was proven. The discovery of fullerenes provided exciting insights into carbon nanostructures and how architectures built from sp^2 carbon units based on simple geometrical principles can result in new symmetries and structures that have fascinating and useful properties (Kroto et al., 1985). Fullerenes are a class of carbon allotropes (Fig. 1), They are molecules composed entirely of carbon, in the form of a hollow sphere, ellipsoid, or tube. Cylindrical fullerenes are called carbon nanotubes or buckytubes. Fullerenes are similar in structure to graphite, which is composed of a sheet of linked hexagonal rings, but they contain pentagonal (or sometimes heptagonal) rings that prevent the sheet from being planar.

Carbon nanotube (CNT) is one form of carbon, with nanometer-sized diameter and micrometer-sized length (where the length to diameter ratio exceeds 1000). The atoms are arranged in hexagons, the same arrangement as in graphite. The structure of CNT consists of enrolled cylindrical graphitic sheet (called graphene) rolled up into a seamless cylinder with diameter of the order of a nanometer. It is understood that CNT is

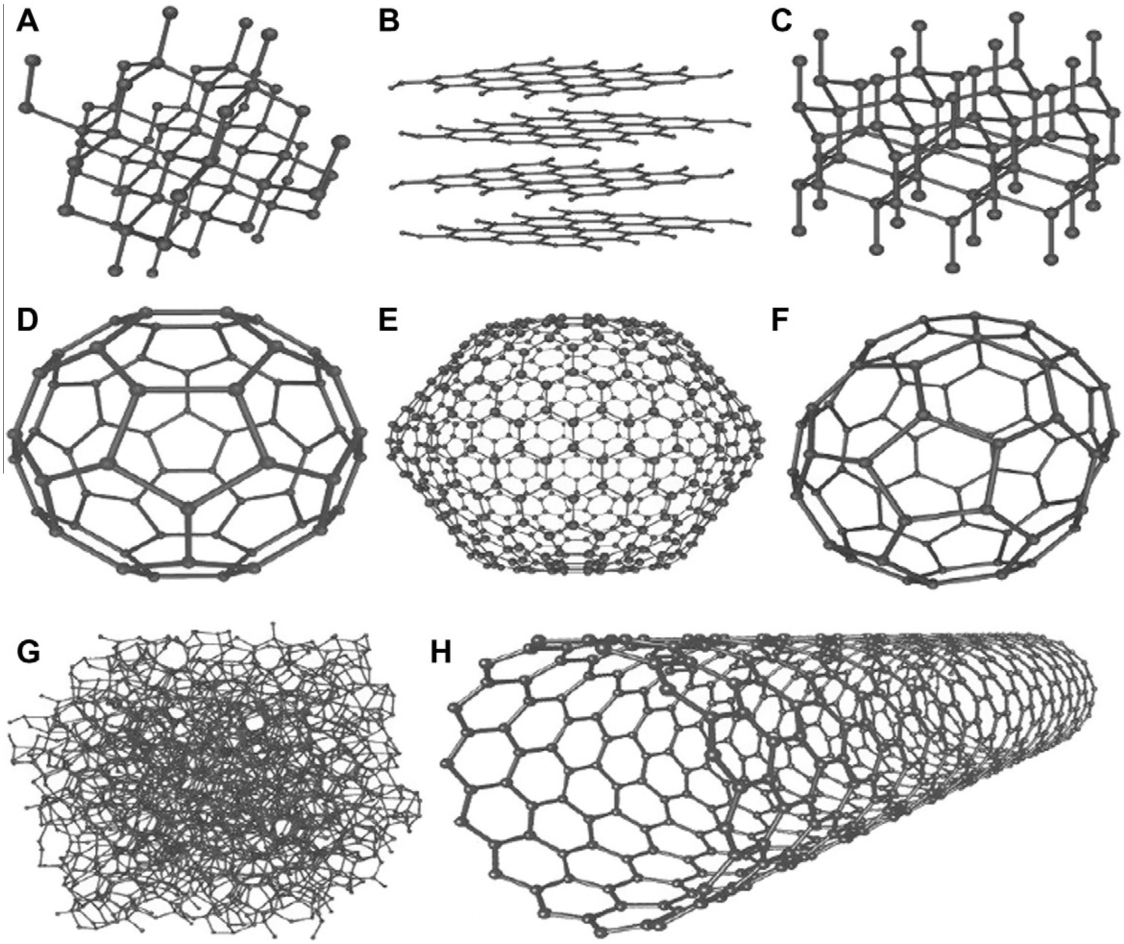

Figure 1 The structures of eight allotropes of carbon: (A) Diamond [3D, network covalent structure], (B) Graphite [2D, covalent plates] (graphene is a single of graphite), (C) Lonsdaleite, (D) C_{60} [0D, molecules] (Buckminsterfullerene or bukyball), (E) C_{540} Fullerene, (F) C_{70} Fullerene, (G) Amorphous carbon, (H) Single-walled carbon nanotube [1D, tubes] (buckytube).

the material lying in between fullerenes and graphite as a quite new member of carbon allotropes (Tanaka et al., 1999).

Carbon nanotubes are members of the fullerene structural family, which also includes buckyballs. Whereas buckyballs are spherical in shape, a CNT is cylindrical, the ends of some CNTs are open; the others are closed with full fullerene caps. CNTs name is derived from their size, since the diameter of a CNT is on the order of a few nanometers (approximately 50,000 times smaller than the width of a human hair), while they can be up to several micrometer in length. Commercial applications for CNT have been rather slow to develop, however, primarily because of the high production costs of the best quality CNTs.

2. History of CNTs

Carbon is known to be the most versatile element that exists on the earth. It has many different properties which can be used in different ways depending on how the carbon atoms are arranged. For more than 6000 years carbon has been used for the reduction of metal oxides. Carbon in the form of graphite was discovered in 1779, and 10 years later in the form of a diamond. It was then determined that both of these forms belong to a family of chemical elements. It was not until about 200 years later that the next advancements in carbon took place. In 1985, Kroto, Smalley, and Curl discovered fullerenes (Kroto et al., 1985), recipients of 1996 Nobel Prize in Chemistry for the discovery of fullerenes. A few years later, CNT was discovered.

The current huge interest in CNTs is a direct consequence of the synthesis of buckminsterfullerene C_{60}, and other fullerenes, in 1985. The discovery that carbon could form stable, ordered structures other than graphite and diamond stimulated researchers worldwide to search for other new forms of carbon. The search was given new impetus when it was shown in 1990 that C_{60} could be produced in a simple arc evaporation apparatus readily available in all laboratories. It was using such an evaporator that the Japanese scientist “Sumio Iijima” discovered fullerene-related CNTs in 1991 (Iijima, 1991). The tubes contained at least two layers (multi-walled carbon nanotubes MWCNTs), often many more, and ranged in outer diameter from about 3 nm to 30 nm. They were invariably closed at both ends.

A scanning of some MWCNT is shown in 1993; a new class of CNT was discovered, with just a single layer. These (single-walled carbon nanotubes SWCNTs) are generally narrower than the multi-walled tubes, with diameters typically in the range 1–2 nm, and tend to be curved rather than straight.

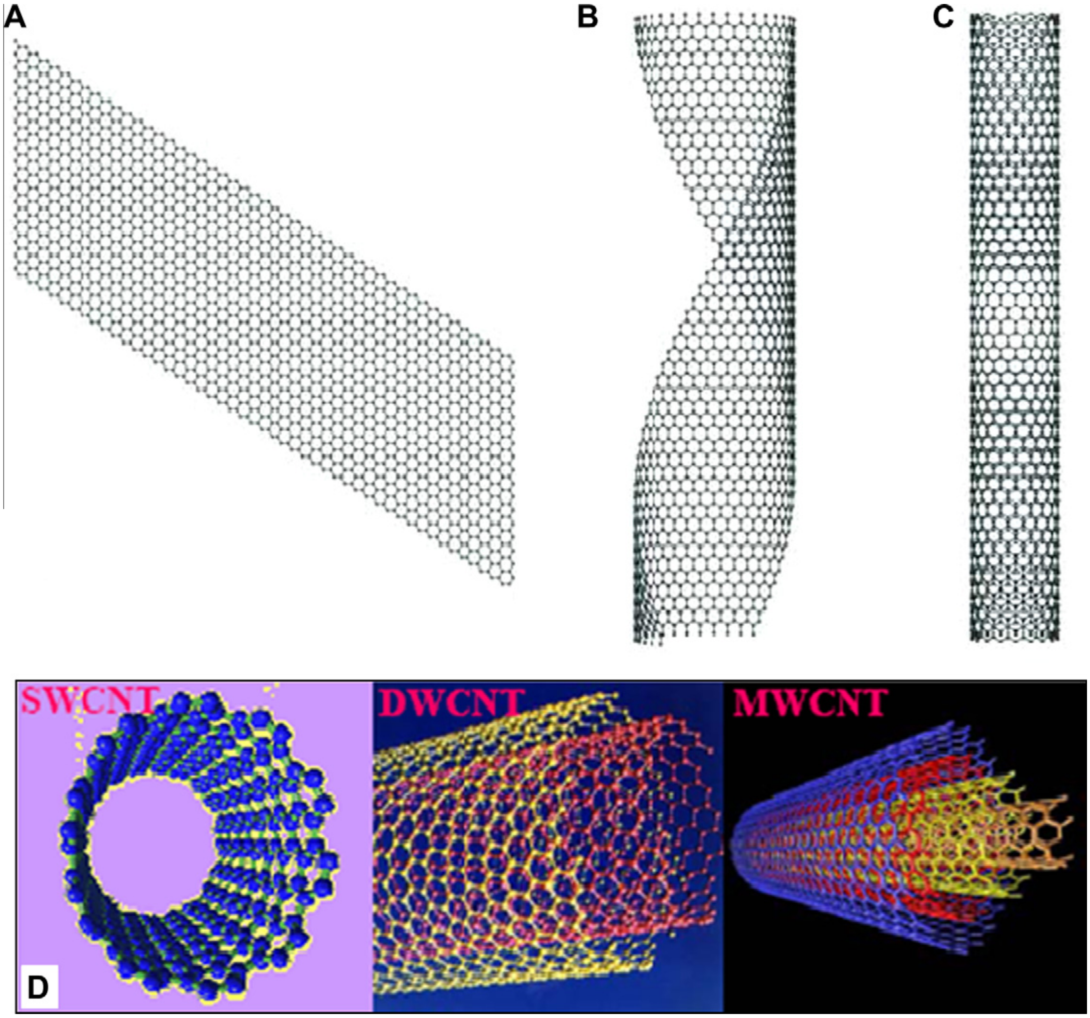

Figure 2 Schematic diagrams showing different types of CNTs and other carbon structures: (A) Flat sheet of Graphite, (B) Partially rolled sheet of graphite, (C) SWCNT, (D) Structures of the three CNT types; SWCNT, DWCNT, and MWCNT, respectively.

It was soon established that these new fibers had a range of exceptional properties, and this lead to increase of research into CNTs. It is important to note, however, that nanoscale tubes of carbon, produced catalytically, had been known for many years before Iijima's discovery. The main reason why these early tubes did not excite wide interest is that they were structurally rather imperfect, so did not have particularly interesting properties. Recent research has focused on improving the quality of produced CNTs (Harris, 2003).

Carbon nanotubes have been produced and observed under a variety of conditions prior to 1991. But many believe that Iijima's report in 1991 is of particular importance because it brought CNTs into the awareness of the scientific community as a whole.

3. Types of CNTs

The two main types of CNT are the single and multi-walled, but there are some other rare types such as fullerite, torus, and nanoknot.

3.1. Single-walled

A single-walled carbon nanotubes (SWCNTs) can be considered to be formed by the rolling of a single layer of graphite (called a graphene layer) into a seamless cylinder (long wrapped graphene sheets). As stated before, CNTs generally have a length to diameter ratio of about 1000 and more so they can be considered as nearly one-dimensional structure. Most SWCNTs have a diameter of close to 1 nm. More detailed, a SWCNT consists of two separate regions with different physical and chemical properties. The first is the sidewall of the tube and the second is the end cap of the tube (Iijima and Ichihashi, 1993).

SWCNTs are a very important variety of a CNT because they exhibit important electric properties that are not shared by the MWCNT variants. The most basic building block of these systems is the electric wire, and SWCNTs can be excellent conductors.

SWCNTs are still very expensive to produce, and the development of more affordable synthesis techniques is vital to the

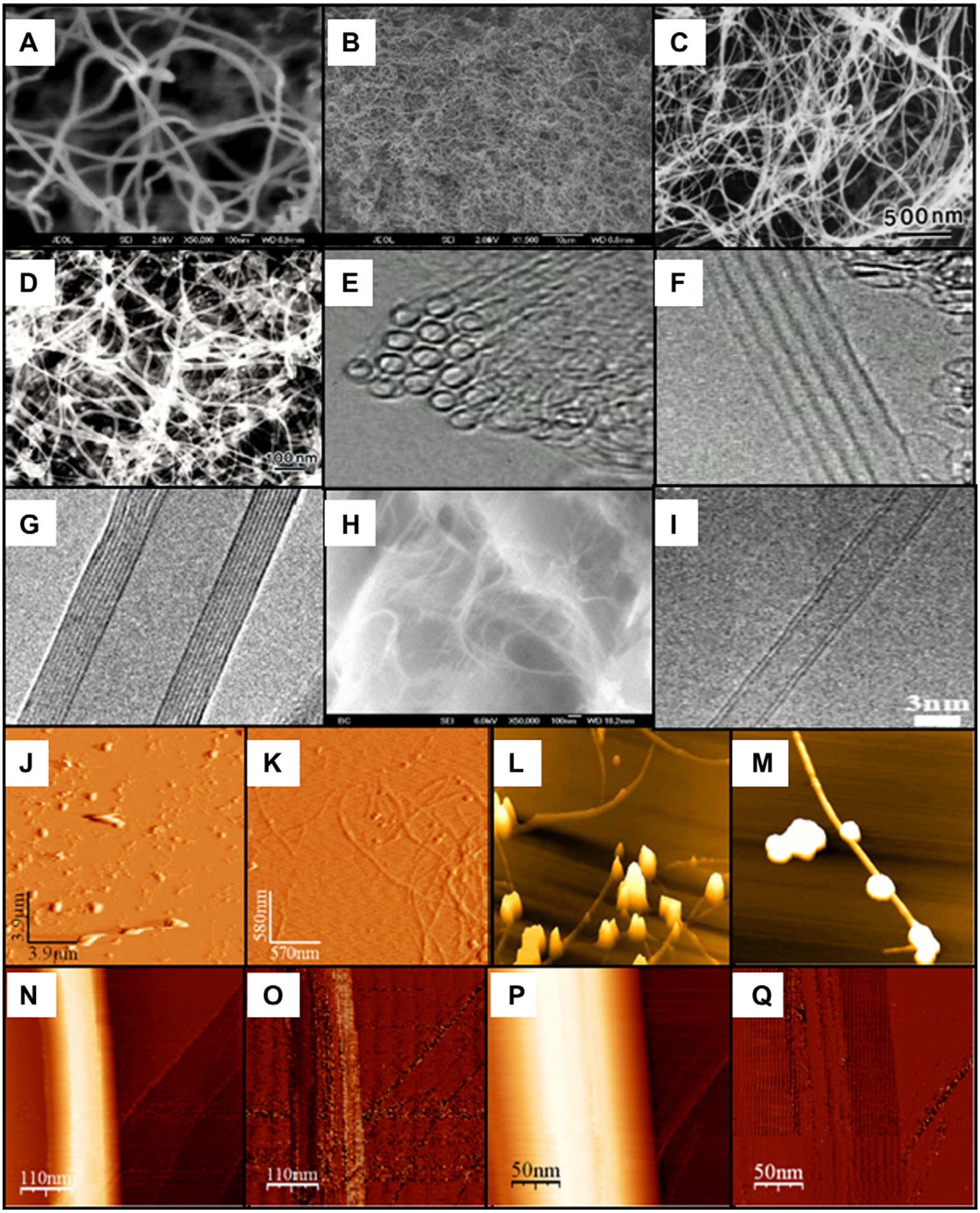

Figure 3 Structure of SWCNT, DWCNT, and MWCNT in different imaging techniques: (A and B) SEM images of MWCNT (high and low magnification), (C and D) SEM images of SWCNT (high and low magnification), (E) TEM image of a cross-sectional view of a bundle of SWCNTs [transverse view shown in (F)]. Each nanotube has a diameter of about 1.4 nm and the tube–tube distance in the bundles is 0.315 nm, (G) High resolution TEM image of an individual MWCNT, (H) SEM image of DWCNT, (I) TEM image of DWCNT, (J) AFM image of MWCNT's on gold surface, [with high magnification in (K)], (L) AFM image of the SWCNT, [with high magnification in (M)], (N) STM image of a MWCNT. Height of the tube is 1.5 nm and the width is 120 nm. [Zoom onto the nanotubes in figure (P)], (O andQ) Current trace of figures (N,P). One can more easily see the appearance of some underlying (Li, 2003; Ren et al., 1998; Nordström and Nyrup, 2004; Safarova et al., 2007).

future of carbon nanotechnology. If cheaper means of synthesis cannot be discovered, it would make it financially impossible to apply this technology to commercial scale applications (Collins and Avouris, 2000).

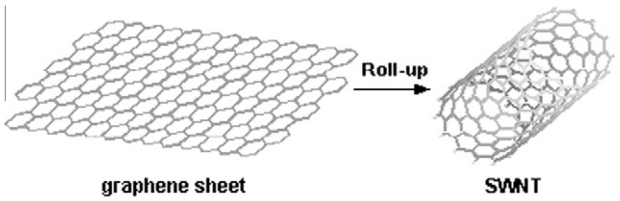

Figure 4 Rolling of a single layer of graphite sheet into SWCNT.

3.2. Multi-walled

Multi-walled carbon nanotubes (MWCNTs) can be considered as a collection of concentric SWCNTs (consist of multiple layers of graphite rolled in on themselves to form a tube shape) with different diameters. The length and diameter of these structures differ a lot from those of SWCNTs and, of course, their properties are also very different (Iijima and Ichihashi, 1993).

The interlayer distance in MWCNTs is close to the distance between graphene layers in graphite, approximately 3.3 Å. The special case of MWCNTs (double-walled carbon nanotubes DWCNTs) must be emphasised here because they combine very similar morphology and properties as compared to SWCNT. DWCNT synthesis on the gram scale was first proposed in 2003 (Flahaut et al., 2003) by the chemical vapour deposition (CVD) technique, from the selective reduction of oxides solid solutions in methane and hydrogen (Figs. 2 and 3).

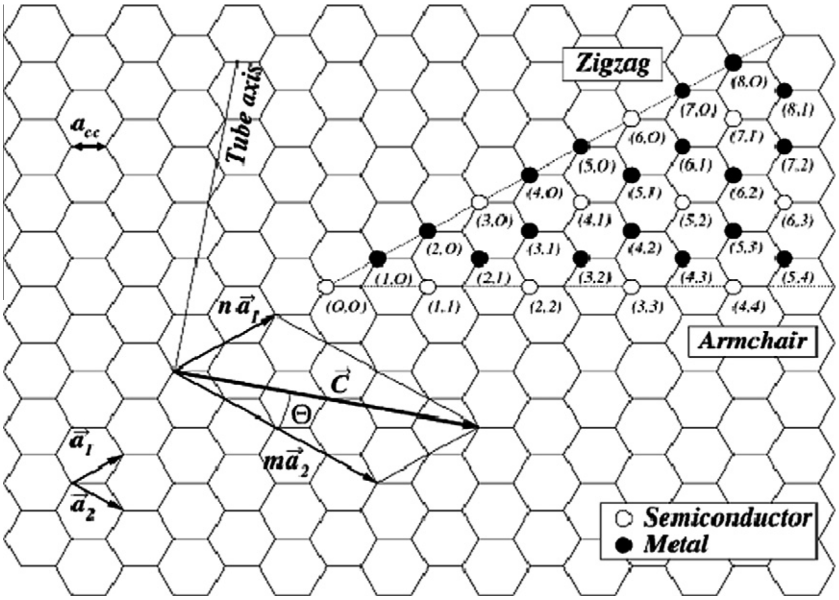

Figure 5 The 2D graphene sheet diagram showing a vector structure classification used to define CNT structure (Dresselhaus et al., 1996).

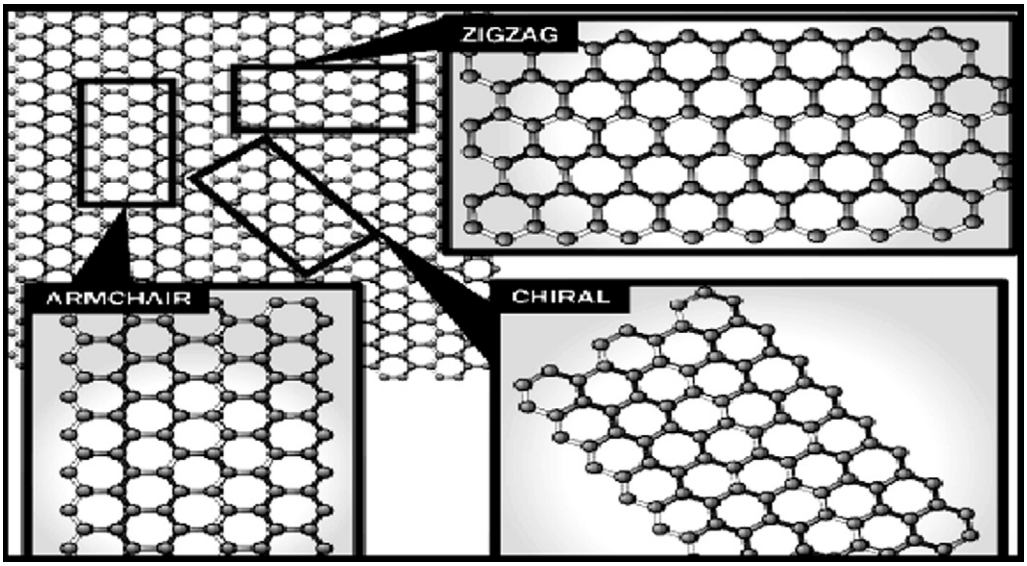

Figure 6 Schematic diagram showing the way of formation different CNTs chirality structures.

4. Structure of CNTs

Carbon nanotubes are sheets of graphite that have been rolled into a tube (Thostenson et al., 2001). A graphene sheet can be in rolled more than one way, producing different types of CNTs, (graphene is an individual graphite layer, Fig. 4).

CNTs are considered as nearly one-dimensional structures (1D buckytube shape) according to their high length to diameter ratio. Most important structures are SWCNTs and MWCNTs. A SWCNT is considered as a cylinder with only one wrapped graphene sheet while MWCNTs are similar to a collection of concentric SWCNTs. The length and diameter of these structures differ a lot from those of SWCNTs and, of course, their properties are also very different. The bondings in CNTs is sp^2 and consist of honeycomb lattices and are seamless structure, with each atom joined to three neighbors, as in graphite. The tubes can therefore be considered as rolled up graphene sheets.

The type of CNT depends on how the graphene sheet is oriented on rolling. This can be specified by a vector (called chiral vector), which defines how the graphene sheet is rolled up. Fig. 5 showing how a hexagonal sheet of graphite is rolled to form a CNT in a vector structure classification.

The vector is determined by two integers (*n*,*m*). Two atoms in a planar graphene sheet are chosen and one is used as origin. The chiral vector *C* is pointed from the first atom toward the second one and is defined by the relation (Dresselhaus et al., 1995):

$$C = na_1 + ma_2$$

Where: *n* and *m* are integers. a_1 and a_2 are the unit cell vectors of the two-dimensional lattice formed by the graphene sheets. The direction of the CNT axis is perpendicular to this chiral vector. For example; to produce a CNT with the indices (6,3), say, the sheet is rolled up so that the atom labelled (0,0) is superimposed on the one labelled (6,3).

The length of the chiral vector *C* is the circumference of the CNT and is given by the corresponding relationship:

$$c = |C| = a\sqrt{(n^2 + nm + m^2)}$$

Where the value *a* is the length of the unit cell vector a_1 or a_2. This length *a* is related to the carbon–carbon bond length a_{cc} by the relation:

$$a = |a_1| = |a_2| = a_{cc}\sqrt{3}$$

For graphite, the carbon–carbon bond length is $a_{cc} = 0.1421$ nm. The same value is often used for CNTs (Wildoer et al., 1998). But due to the curvature of the tube a slightly larger value such as $a_{cc} = 0.144$ nm should be a better approximation (Murakami et al., 2003; Saito et al., 2000; Jorio et al., 2001).

Using the circumferential length *c*, the diameter of the CNT is thus given by the relation:

$$d = c/\pi$$

The angle between the chiral vector and zig-zag nanotube axis is the chiral angle θ. With the integers *n* and *m* already introduced before, this angle can be defined by:

$$\theta = \tan^{-1}(m\sqrt{3})/(m + 2n)$$

Carbon nanotubes are only described by the pair of integers (*n*,*m*) which is related to the chiral vector. It can be seen from Figs. 5–7 three types of CNTs are revealed with these values:

- $m = 0$ for all zig-zag tubes and ($\theta = 30°$);
- $n = $ m for all armchair tubes and ($\theta = 0°$);
- Otherwise, when $n \neq m$ they are called chiral tube and ($0° < \theta < 30°$).

The value of (*n*,*m*) determines the chirality of CNT and affects the optical, mechanical and electronic properties. CNTs with $|n - m| = 3i$ are metallic like as in (10,10) tube, and those with $|n - m| = 3i \pm 1$ are semiconducting like as in (10,0) tube, (*i* is an integer).

The armchair and zig-zag tubes structures have a high degree of symmetry. These terms refer to the arrangement of hexagons around the circumference. While the chiral tube

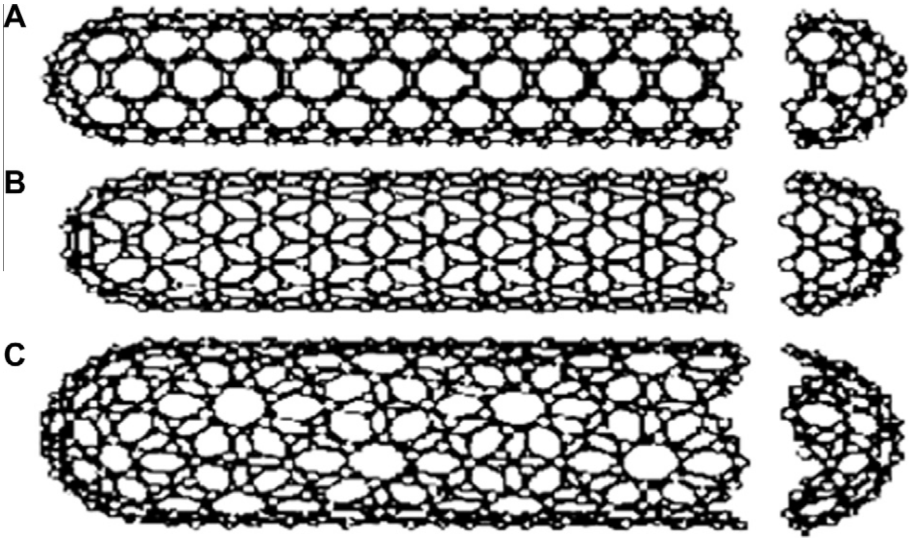

Figure 7 CNTs structure with different chiralities. The difference in structure is easily shown at the open end of the tubes. (A) armchair structure, (B) zig-zag structure, (C) chiral structure.

structure, which in practice is the most common, meaning that it can exist in two mirror-related forms.

The three distinct ways in which a graphene sheet can be rolled into a tube are shown in Fig. 6.

And the CNTs structural types are shown in Fig. 7 (Daenen et al., 2003).

The terminating cap of CNT is formed from pentagons and hexagons. The smallest cap that fits on to the cylinder of the carbon tube seems to be the well-known C_{60} hemisphere. The smallest experimental value of CNT diameter of 0.7 nm is in good agreement with this cap (Dresselhaus et al., 1995). However, some authors have recently studied CNTs at the theoretical limit of 0.4 nm in diameter (Tang et al., 2003; Qin et al., 2000; Liang et al., 2002; Sano et al., 2002; Zhao et al., 2004; Tang et al., 2003; Agrawal et al., 2004; Machon et al., 2002). These CNTs are sometimes capped with a C_{20} dodecahedron (Qin et al., 2000).

Specific surface area gives good information of CNT characteristics and properties. Using some geometrical calculations, the theoretical external specific surface area for CNTs have been determined (Peigney et al., 2001). For one side of graphene sheet, the value obtained is 1315 m^2g^{-1} but using different multi-walled geometries and nanotubes bundles the value decreases to 50 m^2g^{-1}.

The easiest way to visualise how CNTs are built up is to start with graphite, the most stable form of crystalline carbon. Graphite consists of layers of carbon atoms. Within the layers, the atoms are arranged at the corners of hexagons which fill the whole plane (in the idealized case without defects). The carbon atoms are strongly (covalently) bound to each other (carbon–carbon distance ~0.14 nm). The layers themselves are rather weakly bound to each other (weak long-range van der Walls-type interaction, interlayer distance of ~0.34 nm). The weak interlayer coupling gives graphite the property of a seemingly very soft material, the property which allows using graphite in a pen to write with.

The nature of the bonding of a CNT is described by applied quantum chemistry, specifically, orbital hybridisation. The chemical bonding of CNTs is composed entirely of sp^2 bonds, similar to those of graphite. This bonding structure, which is stronger than the sp^3 bonds found in diamond, provides the molecules with their unique strength. CNTs naturally align themselves into ropes held together by van der Waals forces. Under high pressure, CNTs can merge together, trading some sp^2 bonds for sp^3 bonds, giving great possibility for producing strong, unlimited length wires through high pressure CNT linking (Yildirim et al., 2000).

5. Synthesis of CNTs

The way in which CNTs are formed is not exactly known. The growth mechanism is still a subject of study, and more than one mechanism might be operative during the formation of CNTs. One of the mechanisms consists out of three steps. First a precursor to the formation of CNTs and fullerenes, C_2, is formed on the surface of the metal catalyst particle. From this metastable carbide particle, a rod-like carbon is formed rapidly. Secondly there is a slow graphitisation of its wall. This mechanism is based on in situ TEM observations (Ayumu et al., 2002). The exact atmospheric conditions depend on the technique used. The actual growth of the CNT seems to be the same for all techniques mentioned.

The most accepted growth mechanisms are two models: tip-growth (Iijima and Ichihashi, 1993; Thess et al., 1996) and root growth (Saito et al., 1995). In the former, a tubule tip is open so that carbon atoms can be added to its circumference, and the metal catalyst promotes the growth reaction and also prevents the tubule tip closure. One study proposed that fullerene molecules would act as the growth nuclei such that the diameter of the tubule will determine CNT size (Hafner et al., 1998). The latter model is based on the phase diagram of carbon and a metal. The SWCNTs grow as carbon precipitates when the molten metal dissolving carbon is cooled and solidified. More convincing experimental evidence is needed for better understanding of the growth mechanism (Iijima, 1998).

There are several theories on the exact growth mechanism for CNTs. One of the most accepted theories postulates that metal catalyst particles are floating or are supported on graphite or another substrate (Sinnot et al., 1999). It presumes that the catalyst particles are spherical or pear shaped, in which case the deposition will take place on only one half of the surface (this is the lower curvature side for the pear shaped particles). The carbon diffuses along the concentration gradient and precipitates on the opposite half, around and below the bisecting diameter. However, it does not precipitate from the apex of the hemisphere, which accounts for the hollow core that is characteristic of these filaments. For supported metals, filaments can form either by extrusion, in which the CNT grows upwards from the metal particles that remain attached to the substrate, or by tip-growth, in which the particles detach and move at the head of the growing CNT. Depending on the size of the catalyst particles, SWCNT or MWCNT is grown (Fig. 8).

Carbon nanotubes are generally produced by three main techniques: arc discharge, laser ablation, and chemical vapour deposition. Though scientists are researching more economic ways to produce these structures.

In arc discharge technique, a vapor is created by an arc discharge between two carbon electrodes with or without catalyst. CNTs self assemble from the resulting carbon vapour. In the laser ablation technique, a high power laser beam impinges on a volume of carbon containing feedstock gas (such as methane or carbon monoxide). At the moment, laser ablation produces a small amount of clean CNTs, whereas arc discharge methods generally produce large quantities of impure material. In general, chemical vapour deposition (CVD) results in MWCNTs or poor quality SWCNTs. The SWCNTs produced with CVD have a large diameter range, which can be poorly controlled. But on the other hand, this method is very easy to scale up, what favors commercial production (Daenen et al., 2003).

Laser ablation was the first technique used to generate fullerenes in clusters. In this process, a piece of graphite is vaporised by laser irradiation under an inert atmosphere. This results in soot containing CNTs which are cooled at the walls of a quartz tube (Journet and Bernier, 1998).

The CVD and the most current fluidised bed (FB) chemical vapour deposition method has shown the most promise in terms of its price/unit ratio due to excellent heat and mass transfer ensuing a homogeneous product, inherent scalability and comparatively low cost (See and Harris, 2007). CVD generally involves reacting a carbon containing gas (such as

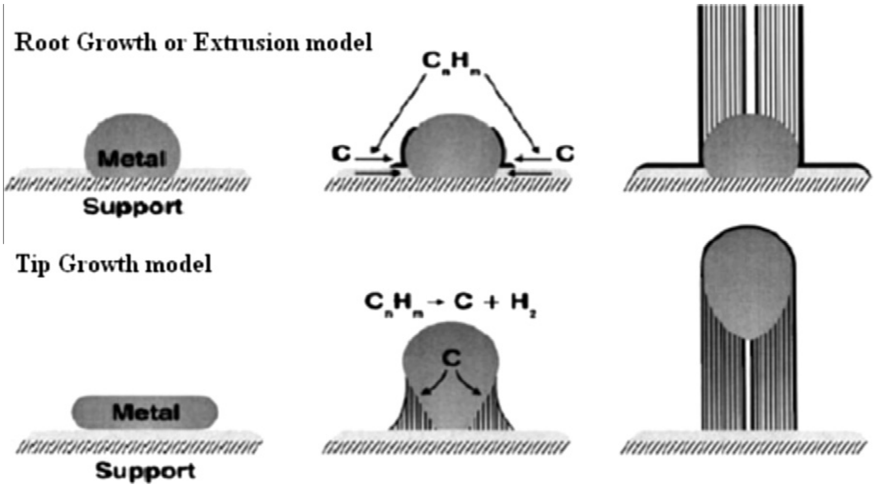

Figure 8 Visualisation of a possible CNT growth mechanism.

acetylene, ethylene, and ethanol) with a metal catalyst particle (usually cobalt, nickel, iron or a combination of these such as cobalt/iron or cobalt/molybdenium) at temperatures above 600 °C. Unfortunately, although these methods can produce large quantities of CNTs, their cost is still high to make any large-scale applications.

Carbon nanotubes were observed in 1991 in the carbon soot of graphite electrodes during an arc discharge, by using a current of 100 amps, which was intended to produce fullerenes (Iijima, 1991). However, the first macroscopic production of CNTs was made in 1992 by two researchers at NEC's Fundamental Research Laboratory (Ebbesen and Ajayan, 1992). The method used was the same as in 1991. During this process, the carbon contained in the negative electrode sublimates because of the high temperatures caused by the discharge. Because CNTs were initially discovered using this technique, it has been the most widely used method of CNT synthesis.

Commonly used gaseous carbon sources include: methane, ethylene, ethanol, carbon monoxide and acetylene. If both electrodes are graphite (pure graphite electrodes), the main product will be MWCNTs. But if SWCNTs are preferable, the anode has to be doped with metal catalyst, such as: Fe, Co, Ni, Y or Mo (use a mixture of graphite with metal catalysts).

In addition to previous methods, high pressure CO disproportionation process (Nikolaev et al., 1999; Bronikowski et al., 2001), flame synthesis (Ayumu et al., 2002; Vander et al., 2001; Wal et al., 2002), plasma torch method (Alford et al., 2001), electrolysis (Hsu et al., 1995), and solar energy (Laplaze et al., 1998) methods have also been proposed to the synthesis of CNTs and specially to the synthesis of SWCNTs.

Fullerenes and CNTs are not necessarily products of high-tech. laboratories; they are commonly formed in such mundane places as ordinary flames (Singer and Grumer, 1959), produced by burning methane (Liming et al., 2001a), ethylene (Liming et al., 2001b), and benzene (Duan and McKinnon, 1994), and they have been found in soot from both indoor and outdoor air (Murr et al., 2004). However, these naturally occurring varieties can be highly irregular in size and quality because the environment in which they are produced is often highly uncontrolled. Thus, although they can be used in some applications, they can lack in the high degree of uniformity necessary to meet many needs of both research and industry. Table 1 summarises the three most common techniques used.

Currently, a CVD is the most widely used method to produce the CNTs, other methods had been recently developed for the preparation of CNTs and improving the existing methods, promising results have been achieved for reaching the better degree of purification and effectively reducing the treatment time (Liu and Harris, 2008; MacKenzie et al., 2009; Liu et al., 2008; Barkauskas et al., 2010).

Some of the CNTs preparation methods are more effective than others but a problem that all methods face is the ability of the CNTs to self align. Many applications of CNTs require controlled growth of aligned CNTs with surface modification. Controlled synthesis of well-aligned CNTs in predetermined patterns is particularly important in terms of fundamental studies and applications (Paradise and Goswami, 2007; Dai, 2002) (Fig. 9A and B).

6. Purification of CNTs

A large problem with CNT application is next to large-scale synthesis and also the purification. In all the CNT preparation methods, the CNTs come with a number of impurities whose type and amount depend on the technique used. The most common impurities are carbonaceous materials, whereas metals are the other types of impurities generally observed (Ebbesen, 1997).

The as-produced CNT soot contains a lot of impurities. The main impurities in the soot are graphite (wrapped up) sheets, amorphous carbon, metal catalyst and the smaller fullerenes. These impurities will interfere with most of the desired properties of the CNTs. Also in the fundamental research, it is preferred to obtain CNTs, as pure as possible. In order to understand the measurements better, the CNT samples also have to be as homogeneous as possible. The common industrial techniques use strong oxidation and acid-refluxing techniques, which have an effect on the structure of the tubes. Purification difficulties are considerable because CNTs are insoluble and, hence, liquid chromatography is limited.

Table 1 A summary of the major production methods and their efficiency.

Method	Arc discharge method	Chemical vapour deposition	Laser ablation (vaporisation)
Who	Ebbesen and Ajayan, NEC, Japan 1992 (Ebbesen and Ajayan, 1992)	Endo, Shinshu University, Nagano, Japan (Morinobu et al., 1993)	Smalley, Rice, 1995 (Jung et al., 2003)
How	Connect two graphite rods to a power supply, place them a few millimeters apart, and throw the switch. At 100 amps, carbon vaporises and forms hot plasma	Place substrate in oven, heat to 600 °C, and slowly add a carbon bearing gas such as methane. As gas decomposes it frees up carbon atoms, which recombine in the form of CNTs	Blast graphite with intense laser pulses; use the laser pulses rather than electricity to generate carbon gas from which the CNTs form; try various conditions until hit on one that produces prodigious amounts of SWCNTs
Typical yield	30–90%	20–100%	Up to 70%
SWCNTs	Short tubes with diameters of 0.6–1.4 nm	Long tubes with diameters ranging from 0.6 to 4 nm	Long bundles of tubes (5–20 microns), with individual diameter from 1 to 2 nm
MWCNTs	Short tubes with inner diameter of 1–3 nm and outer diameter of approximately 10 nm	Long tubes with diameter ranging from 10 to 240 nm	Not very much interest in this technique, as it is too expensive, but MWCNT synthesis is possible
Production	Can easily produce SWCNT, MWCNTs. SWCNTs have few structural defects; MWCNTs without catalyst, not too expensive, open air synthesis possible	Easiest to scale up to industrial production; long length, simple process, SWCNT diameter controllable, quite pure	Primarily SWCNTs, with good diameter control and few defects. The reaction product is quite pure
Defects	Tubes tend to be short with random sizes and directions; often needs a lot of purification	CNTs are usually MWCNTs and often riddled with defects	Costly technique, because it requires expensive lasers and high power requirement, but is improving
Schematic diagram	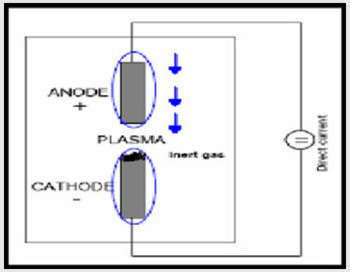	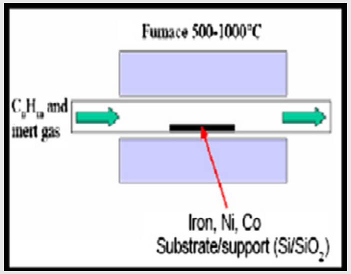	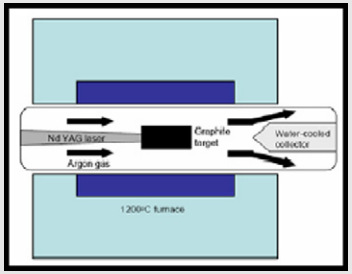
References	Collins and Avouris (2000), Ebbesen and Ajayan (1992), Journet and Bernier (1998)	Ren et al. (1998), Ren et al. (1999), Masako et al. (1995), Masako et al. (1997), Sinnot et al. (1999), Jose-Yacaman et al. (1993), Ren et al. (1998)	Collins and Avouris (2000), Guo et al. (1995), Yudasaka et al. (1999), Eklund et al. (2002), Maser et al. (1998), Bolshakov et al. (2002), Scott et al. (2001), Guo et al. (1995)

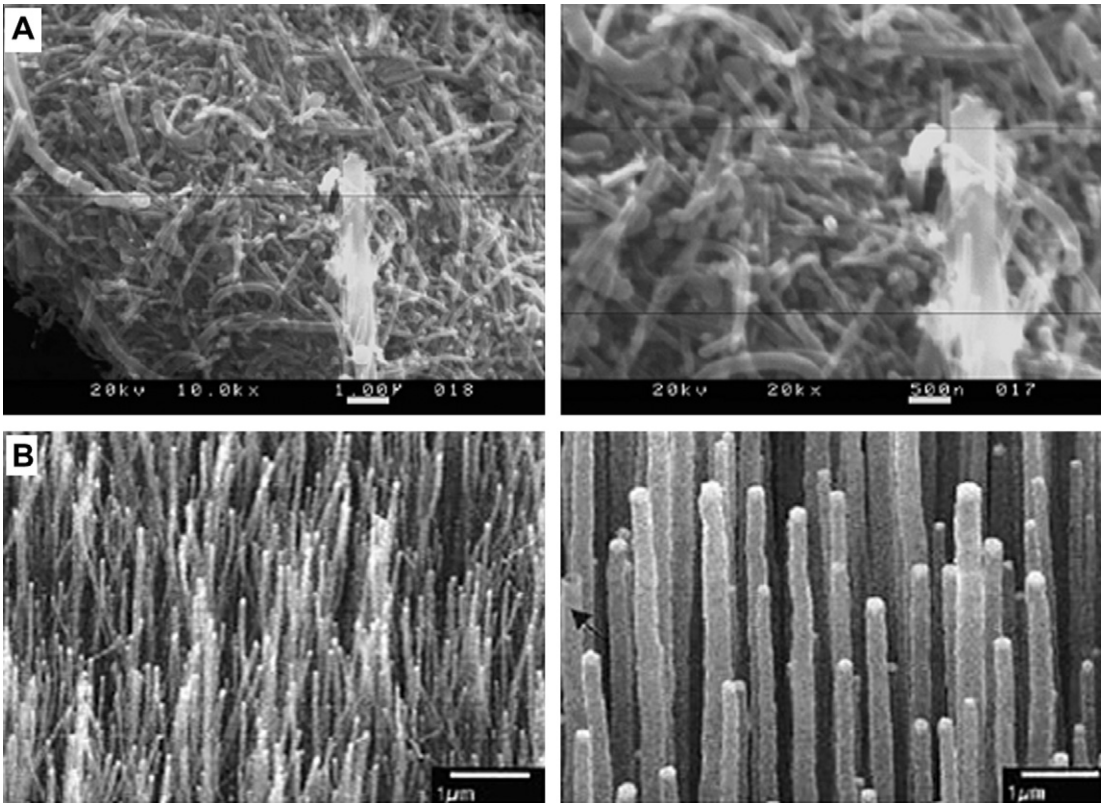

Figure 9 (A) Scanning electron micrographs of CNTs at 10,000 and 20,000 magnification. (B) Micrographs showing aligned CNTs.

Carbon nanotube purification step (depending on the type of the purification) removes amorphous carbon from CNTs, improves surface area, increases or decreases mesopore or micropore volume, decomposes functional groups blocking the entrance of the pores or induces additional functional groups. In case of adsorption of bacteria for example, CNT purification steps such as heat treatment, NH_3 treatment may be adapted so as to increase surface area and mesopore volume. Basically, these techniques can be divided into two main streams of separation techniques, namely, structure-selective and size-selective separations. The first one will separate the CNTs from the impurities; the second one will give a more homogeneous diameter or size distribution. Most of this techniques used, are combined with other techniques to improve the purification and to remove different impurities at the same time. These techniques are:

6.1. Oxidation

Oxidative treatment of the CNTs is a good way to remove carbonaceous impurities (Hajime et al., 2002; Borowiak-Palen et al., 2002; Huang and Dai, 2002; Chiang et al., 2001; Harutyunyan et al., 2002; Farkas et al., 2002) or to clear the metal surface (Hajime et al., 2002; Chiang et al., 2001; Harutyunyan et al., 2002; Xiang et al., 2001; Kajiura et al., 2002; Moon et al., 2001; Chiang et al., 2001). The main disadvantages of oxidation are that not only the impurities are oxidised, but also the CNTs. Luckily the damage to CNTs is less than the damage to the impurities. These impurities have relatively more defects or a more open structure. Another reason why impurity oxidation is preferred is that these impurities are most commonly attached to the metal catalyst, which also acts as oxidising catalyst (Hajime et al., 2002; Borowiak-Palen et al., 2002; Chiang et al., 2001; Xiang et al., 2001; Houjin et al., 2001). Altogether, the efficiency and yield of the procedure are highly depending on a lot of factors, such as metal content, oxidation time, environment, oxidising agent and temperature.

6.2. Acid treatment

In general, the acid treatment will remove the metal catalyst. First of all, the surface of the metal must be exposed by oxidation or sonication. The metal catalyst is then exposed to acid and solvated. The CNTs remain in suspended form. When using a treatment in HNO_3, the acid only has an effect on the metal catalyst. It has no effect on the CNTs and other carbon particles (Hajime et al., 2002; Borowiak-Palen et al., 2002; Farkas et al., 2002; Kajiura et al., 2002). If a treatment in HCl is used, the acid has also a little effect on the CNTs and other carbon particles (Hajime et al., 2002; Chiang et al., 2001; Moon et al., 2001; Chiang et al., 2001). The mild acid treatment (Bandow et al., 1997) (4 M HCl reflux) is basically the same as the HNO_3 reflux, but here the metal has to be totally exposed to the acid to solvate it (Fig. 10).

A review of the literature demonstrates that the effect of key variables such as acid type and concentration, temperature, duration and pressure are not well understood and, due to their dependence, must be probed with correct experimental design to elucidate potential interaction effects (MacKenzie et al., 2009).

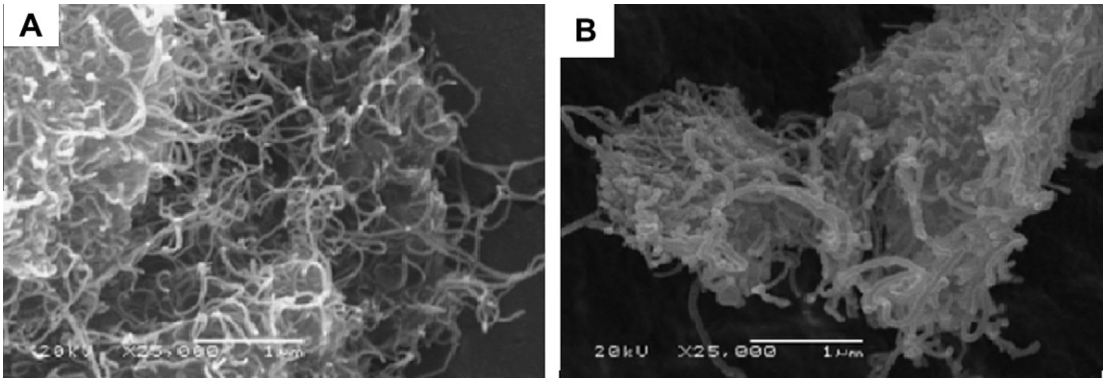

Figure 10 Scanning electron micrographs of raw MWCNTs (A) and oxidised MWCNTs with concentrated HNO3, (B) The images were amplified 25,000 times.

6.3. Annealing and thermal treatment

Due to high temperatures (873–1873 K), CNTs will be rearranged and defects will be consumed (Borowiak-Palen et al., 2002; Chiang et al., 2001; Chiang et al., 2001; Georgakilas et al., 2002). High temperature also causes the graphitic carbon and the short fullerenes to pyrolyse. When using high temperature vacuum treatment (1873 K) the metal will be melted and can also be removed (Kajiura et al., 2002).

6.4. Ultrasonication

This technique is based on the separation of particles due to ultrasonic vibrations. Agglomerates of different nanoparticles will be forced to vibrate and will become more dispersed. The separation of the particles is highly dependable on the surfactant, solvent and reagent used. The solvent influences the stability of the dispersed tubes in the system. In poor solvents the CNTs are more stable if they are still attached to the metal. But in some solvents, such as alcohols, monodispersed particles are relatively stable (Hajime et al., 2002; Xiang et al., 2001; Houjin et al., 2001; Bandow et al., 1997; Shelimov et al., 1998).

When an acid is used, the purity of the CNTs depends on the exposure time. When the tubes are exposed to the acid for a short time, only the metal solvates, but for a longer exposure time, the tubes will also be chemically cut (Chiang et al., 2001; Farkas et al., 2002; Chiang et al., 2001).

6.5. Magnetic purification

In this method ferromagnetic (catalytic) particles are mechanically removed from their graphitic shells (Thien-Nga et al., 2002). The CNTs suspension is mixed with inorganic nanoparticles (mainly ZrO_2 or $CaCO_3$) in an ultrasonic bath to remove the ferromagnetic particles. Then, the particles are trapped with permanent magnetic poles. After a subsequent chemical treatment, a high purity CNT material will be obtained (Fig. 11).

This process does not require large equipment and enables the production of laboratory-sized quantities of CNTs containing no magnetic impurities.

6.6. Micro-filtration

Micro-filtration is based on size or particle separation. CNTs and a small amount of carbon nanoparticles are trapped in a filter. The other nanoparticles (catalyst metal, fullerenes and carbon nanoparticles) are passing through the filter (Borowiak-Palen et al., 2002; Moon et al., 2001; Chiang et al., 2001; Houjin et al., 2001; Bandow et al., 1997; Shelimov et al., 1998).

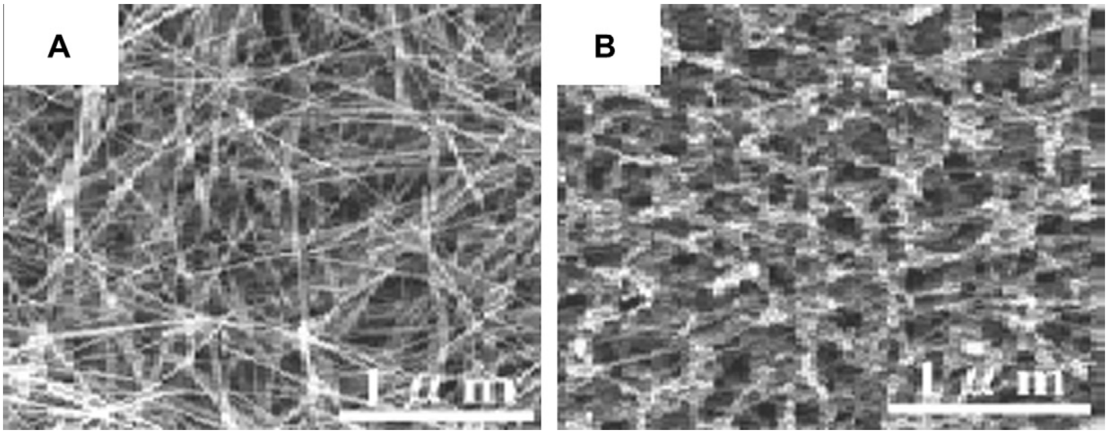

Figure 11 SEM images of MWCNTs synthesised with (A) and without (B) the magnetic field.

One way of separating fullerenes from the CNTs by microfiltration is to soak the as-produced CNTs first in a CS_2 solution. The CS_2 insoluble are then trapped in a filter. The fullerenes which are solvated in the CS_2, pass through the filter (Bandow et al., 1997).

A special form of filtration is cross flow filtration. In this method the membrane is a hollow fiber. The membrane is permeable to the solution. The filtrate is pumped down the bore of the fiber at some head pressure from a reservoir and the major fraction of the fast flowing solution which does not permeate out the sides of the fiber is fed back into the same reservoir to be cycled through the fiber repeatedly. A fast hydrodynamic flow down the fiber bore (cross flow) sweeps the membrane surface preventing the buildup of a filter cake (Borowiak-Palen et al., 2002; Farkas et al., 2002).

6.7. Cutting

Cutting of the CNTs can either be induced chemically (Gu et al., 2002), mechanically (Gao et al., 2000) or as a combination of these (Farkas et al., 2002).

Carbon nanotubes can be chemically cut by partially functionalising the tubes, for example with fluor (Gu et al., 2002). Then, the fluorated carbon will be driven off the sidewall with pyrolisation in the form of CF_4 or COF_2. This will leave behind the chemically cut CNTs. Mechanical cutting of the CNTs can be induced by ball milling. Here, the bonds will break due to the high friction between the nanoparticles and the CNTs will be disordered (Gao et al., 2000).

A combination of mechanical and chemical cutting of the CNTs is ultrasonically induced cutting in an acid solution (Farkas et al., 2002). In this way the ultrasonic vibration will give the CNTs sufficient energy to leave the catalyst surface. Then, in combination with acid the CNTs will rupture at the defect sites.

6.8. Functionalisation

Functionalisation is based on making CNTs more soluble than the impurities by attaching other groups to the tubes. And this will make it easy to separate from insoluble impurities, such as metal, this method is usually doing with filtration (Niyogi et al., 2001; Zhao et al., 2001). Another functionalisation technique also leaves the CNT structure intact and makes them soluble for chromatographic size separation (Georgakilas et al., 2002). For recovery of the purified CNTs, the functional groups can be simply removed by thermal treatment, such as annealing.

6.9. Chromatography

This technique is mainly used to separate small quantities of CNTs into fractions with small length and diameter distribution. The CNTs are run over a column with a porous material, through which the CNTs will flow. The columns used are Gel Permeation Chromatography (GPC) and High Performance Liquid Chromatography–Size Exclusion Chromatography (HPLC–SEC) columns. The number of pores the CNTs will flow through depends on their size. This means that, the smaller the molecule, the longer the pathway to the end of the column will be and that the larger molecules will come off first. The pore size will control what size distribution can be separated. However, a problem is that the CNTs have to be either dispersed (Farkas et al., 2002) or solvated (Niyogi et al., 2001; Zhao et al., 2001). This can be done by ultrasonication (Farkas et al., 2002) or functionalisation with soluble groups (Niyogi et al., 2001; Zhao et al., 2001). In addition to these purification techniques, CNT has been purified by treating with basic compounds such as KOH, and NH_3 (Chen et al., 2006; Lee et al., 2005; Liu et al., 2006; Niu et al., 2007) and gaseous compounds such as air, CO_2, and ozone (Chen et al., 2006).

With the different techniques for purification, there will be different results achieved. Care should be taken when the technique is chosen, as the effect on the entire sample will also depend on the composition and the amount of the sample. What is desired are techniques that only tear down the carbon impurities and the metals, without changing the CNTs. Sometimes extra care should be taken in adjusting the process variables such as temperature, scale and time. Economically feasible large-scale production and purification techniques are still under development.

As a concluding remark, the above-mentioned purification methods change the structural surfaces of CNTs. As a result, there may be change in some of purified CNT properties. Therefore, the main thrust of the research should be in the area of producing purified CNTs in a single step process to conserve the fascinating features of CNTs.

7. Characterisation of CNTs

There are many production methods for CNTs, each producing material that is slightly different: different in diameter, length, chirality, purity, catalysts, impurity species, and defects. And, although purification methods increase the fraction of CNTs in the sample, it also modifies the CNT themselves: it may open both or one on CNT ends, reduced length, modify functional groups, and sometimes it cause defects (Hu et al., 2001; Mawhinney et al., 2000).

Carbon nanotubes are nanometric carbon particles with a graphitic structure, but it also contains many of the impurities. Characterisation of CNTs to determine the quantity, quality, and properties of the CNTs in the sample is very important, because its applications will require certification of properties and function (Kingston, 2007).

Production of CNTs in a controlled way and in large amount encounters problems, which remains to be solved. It is needed to identify all properties of these tubes. In order to investigate the morphological and structural characterisations of CNTs, a reduced number of techniques could be used. However, to fully characterise CNTs, there are not so many techniques available at the individual level such as scanning tunneling microscopy and transmission electronic microscopy. X-ray photoelectron spectroscopy is helpful in order to determine the chemical structure of nanotubes while neutron and X-ray diffraction, infrared and Raman spectroscopy are mostly global characterisation techniques.

7.1. Photoluminescence spectroscopy

SWCNTs could be either metallic or semiconducting type. The energy gap of the semiconducting tubes is related to the chirality (Ouyang et al., 2001; Lauret et al., 2004) and is approximately proportional to the inverse of the tube diameter (Liu et al., 2002).

SWCNTs are generally grouped in bundles and the interaction between the nanotubes is Van der Waals force. Few CNTs in these bundles are metallic and are similar to nonradiative channels. However, photoluminescence from the recombination electron hole pairs at the band gap has to be expected.

In the semiconducting tubes, the luminescence of these bundles is relaxed inside these channels. Often, due to this interaction between semiconducting and metallic CNTs, no photoluminescence signal is obtained. In order to observe the photoluminescence phenomenon, the bundles must be separated into individual tubes. Some treatments could be used to achieve this separation. One of the most popular techniques is the ultrasonication treatment of the CNTs with surfactants in water suspension such as the SDS (sodium dodecyl sulfate) (Lauret et al., 2004; Lefebvre et al., 2004; Weisman et al., 2004; O'Connell et al., 2003; Lebedkin et al., 2003), and zeolite (Guo et al., 2004).

Carbon atoms in CNTs have *p* electrons which give a large π-electrons system. Fig. 12 show Van Hove singularities in the density of electronic states of these particular π-electrons systems. All the optical spectroscopy of the semiconducting tubes to transitions between the corresponding Van Hove singularities in the valence and conductance band are attributed (Weisman et al., 2004). These transitions are called E_{11}, E_{22}, in the Figure.

The only possible photoluminescence emission here is with E_{11} transition while a wide range of wavelength is useful for the photoluminescence excitation. The energy of the Van Hove singularities maxima is mainly dependent on the CNT diameter (O'Connell et al., 2003). Thus, different (*n*,*m*) SWCNTs in a sample will show various superpositions of distinct E_{xx} transitions which will appear with different wavelengths (Miyauchi et al., 2004). As a consequence, the nature (semiconducting or not), the geometries and the diameters could be accessible using the photoluminescence technique. Moreover, the luminescence spectra seem to be very sensitive to the presence of chemical defects and to the purity of the samples (Lauret et al., 2004).

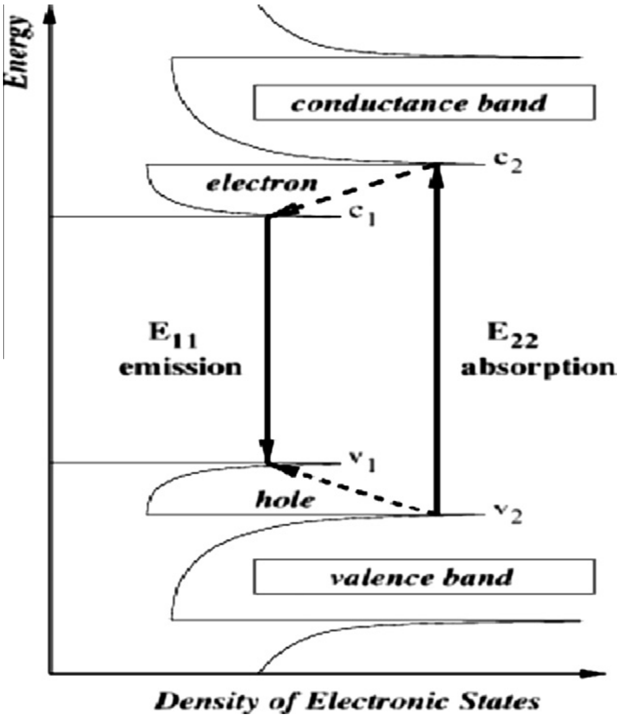

Figure 12 A scheme of photoluminescence excitation for a semiconducting SWCNT. The valence and conductance Van Hove singularities are labelled with the sub band index. The dashed lines show nonradiative transitions for electrons and holes. Optical transitions E_{11} and E_{22} are also represented.

7.2. X-ray photoelectron spectroscopy (XPS)

This technique can give information about the chemical structure of CNTs. But the most widely used data refers to the structure modification of the CNT walls due to the chemical interaction with organic compounds or gases adsorption. CNTs have been studied by XPS the incorporation of nitrogen into CNTs (Droppa et al., 2002). The tip-shift of the peak before and after modification, due to the polar character of the carbon nitrogen bond, is an evidence of the incorporation of nitrogen into the CNT structure (Hammer et al., 2000). This technique also proves that carbon nanofiber material is more like a carbon oxide than a variety of graphite (Pham-Huu et al., 2002).

Studying the sidewall functionalisation of SWCNTs by fluorination is also performed using XPS, which concludes that the C1s of undoped SWCNTs is composed of three peaks: sp^2 carbon (peak at about 284.3 eV), sp^3 carbon (285 eV) and oxygen-related groups (carboxyl) at about 288.5 eV (similar to those observed in nanofibers) (Lee et al., 2003).

In another way, some experiments on 15–20 nm in diameter MWCNTs were also performed (Chen et al., 1999), and revealed the relative differences between the graphite and the CNTs in the C1s peak energy position, the full width at half maximum, and its energy loss fine structures. The C1s of graphite is usually observed at 284.6 eV. However, a negative shift of 0.3 eV observed in the binding energy of these MWCNTs was explained by the weaker C–C bonds resulting from the curvature of the graphene sheets and by the larger interlayer spacing. With MWCNTs of 30 nm in diameter aligned along their tube axis and using spatially resolved XPS, the shift of the C1s binding energy is only about 50 meV between the tips and the sidewalls (Suzuki et al., 2002). The strong influence of structural defects on the electronic structure of MWCNTs explains this difference.

7.3. Electron microscopy (SEM & TEM)

Electron microscopy (scanning and transmission electron microscopy) is an essential tool for characterising any nanomaterial; it gives direct observation of size, shape, and structure (Figs. 13 and 14).

By using the intensity across a CNT section and based on Lambert's law model it is clear that TEM technique is useful for measurement of the outer and inner radius and linear electron absorption coefficient of MWCNTs (Gommes et al., 2003). This method was used to study MWCNTs before and after annealing and noticed a significant increase of the electron absorption coefficient; this increase can be explained by a more structured arrangement of the wall material.

High resolution TEM images was also used for studying the intershell spacing of MWCNTs (Kiang et al., 1998). The intershell spacing is found to range from 0.34 to 0.39 nm varying

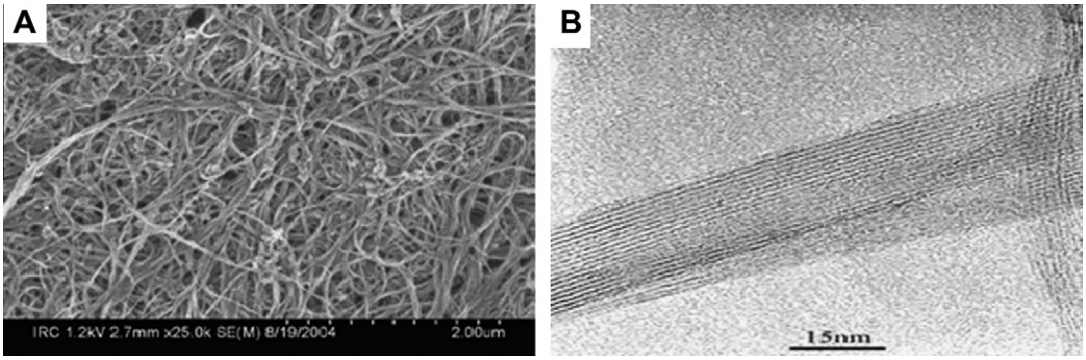

Figure 13 Electron micrographs of SWCNT (Kingston et al., 2004). (A) SEM of SWCNT. (B) TEM of SWCNT.

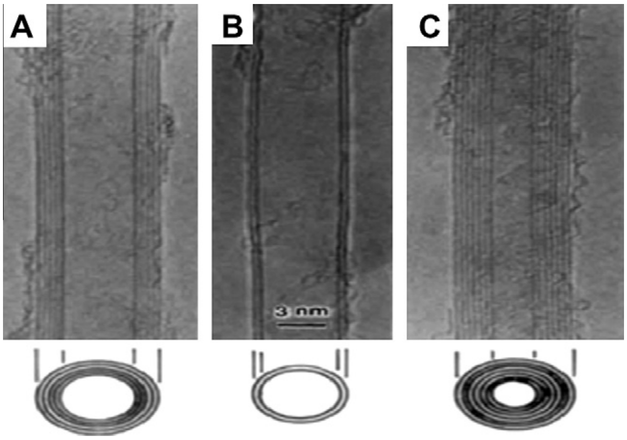

Figure 14 Electron micrographs obtained in the first report of CNTs (Iijima, 1991). Parallel dark lines correspond to the (0 0 2) lattice images of graphite. A cross-section of each tubule is illustrated. (A) Tube consisting of five graphitic sheets, diameter 6.7 nm. (B) Two sheets tube, diameter 5.5 nm. (C) Seven sheet tube, diameter 6.5 nm, which has the smallest hollow diameter (2.2 nm).

with CNT diameter (Fig. 15A–C). However, these values are somewhat greater than the graphite interplanar distance (0.336 nm) (Charlier et al., 1999). This increase is probably due to the curvature of the graphene sheets which is modified by the tube radius. This curvature leads to an increase of the repulsive force and the size effect is more intense in the small diameter (below 10 nm).

7.4. Scanning tunneling microscopy (STM)

Studying the electronic properties of SWCNTs, scientists have been able to calculate models for energy bands and Density of States (DOS) in SWCNTs. If these models have to be experimentally confirmed, a way has to be found in which atomic structures and electron densities can be visualised. STM can do this job as it can display atomic structures as well as measure the DOS (Ouyang et al., 2002).

As is shown in Fig. 16A–C, chirality can clearly be determined from STM measurements. Combining this fact with the ability to measure electronic properties allows studying the effect of CNT chirality on electronic properties. The spectroscopic image (Fig. 16B) shows the DOS as measured by a STM. As these images show, this technique can also be used to determine properties of intramolecular SWCNT junctions. In addition, it can also be used for measuring influence of symmetry, defects, doping, electronic contacts and so on.

To use this technique, CNTs must be deposited on a flat conducting substrate such as HOPG (Sattler, 1995; Ichimura et al., 2002; Lin et al., 1996) or Au (Wildoer et al., 1998; Hassanien and Tokumoto, 2004; Obraztsova et al., 1999; Kim et al., 2000). STM images give directly the three-dimensional morphology of tubes which are consistent with the structure inferred from SEM (Sattler, 1995). Moreover, STM can resolve simultaneously both the atomic structure and the electronic DOS. Thus, this technique is suitable for the CNT characterisation. Experiments to determine atomic structure of SWCNTs were realised at low temperatures (4.2 K) Wildoer et al., 1998, and (77 K) (Ichimura et al., 2002; Kim et al., 2000; Odom et al., 1998). The atomic structure of SWCNTs on top of a rope was also obtained by various authors (Obraztsova et al., 1999; Clauss et al., 1998). These studies confirmed the predicted behaviors of SWCNTs (Hamada et al., 1992; Mintmire et al., 1992; Saito et al., 1992) and revealed the sensitivity of the electronic properties to the helicity and tube diameter.

Using computer simulations, STM images of both metallic and semiconductor SWCNTs with atomic vacancies was predicted (Krasheninnikov, 2001). On STM images, the vacancies resulted in hillock-like features with lateral size of 0.5–0.8 nm (depending on CNTs chirality) and height up to 0.1 nm. A comparison of the electronic superstructure near vacancy can be done with that observed on graphite near point defect.

7.5. X-ray diffraction (XRD)

This technique is used to obtain some information on the interlayer spacing, the structural strain and the impurities. However, CNTs have multiple orientations compared to the X-ray incident beam. Diameters and chiralities distribution are also observed as well as various number of layers for MWCNTs. This leads to a statistical characterisation of CNTs.

The main features of XRD pattern of CNTs are close to those of graphite due to their intrinsic nature, Fig. 17 show the XRD pattern of MWCNT synthesised by CVD method, a graphite-like peak (0 0 2 *l*) is present and measurements of interlayer spacing can be obtained from its position using the

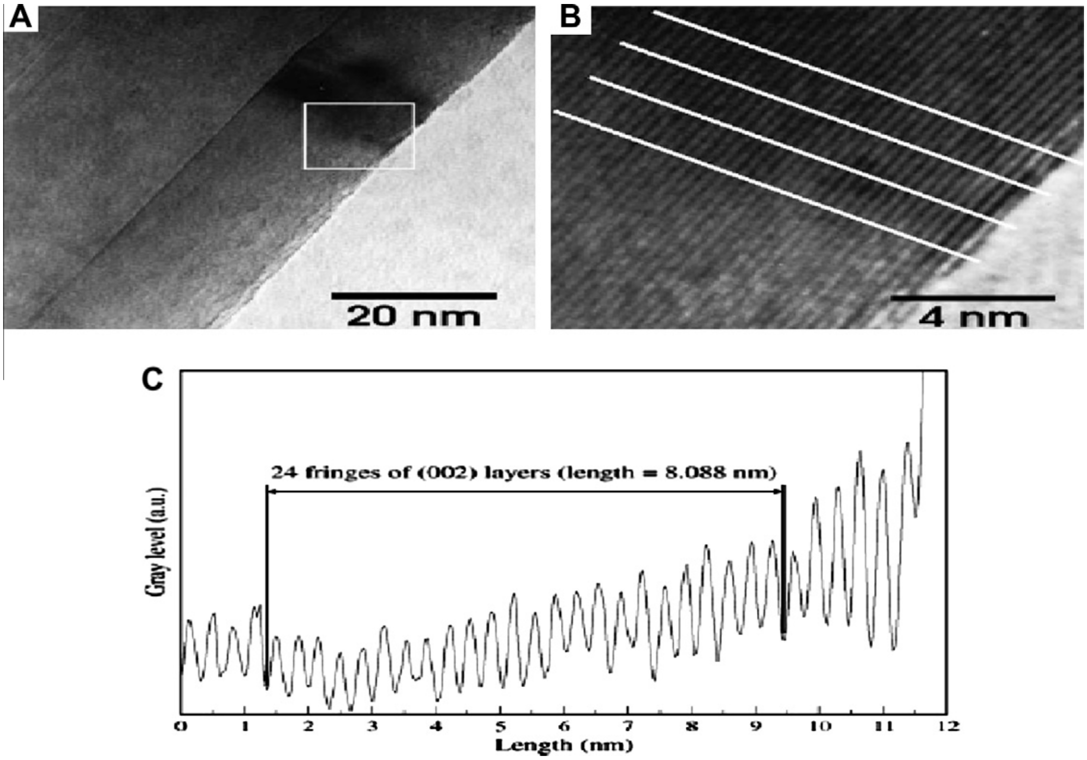

Figure 15 (A) TEM image of a MWCNT (diameter of about 65 nm). These MWCNTs were produced by CVD followed by several oxidation processes. Contrast of the walls are visible. (B) Enlargement of the walls of the CNT. White lines are used in determination for the intershell spacing. (C) Mean profile of the intensity levels of the walls showing the fringes of the (0 0 2) layers used in the determination of the intershell spacing. Here, the value of the intershell spacing is 0.337 ± 0.023 nm and is really close to the graphite one.

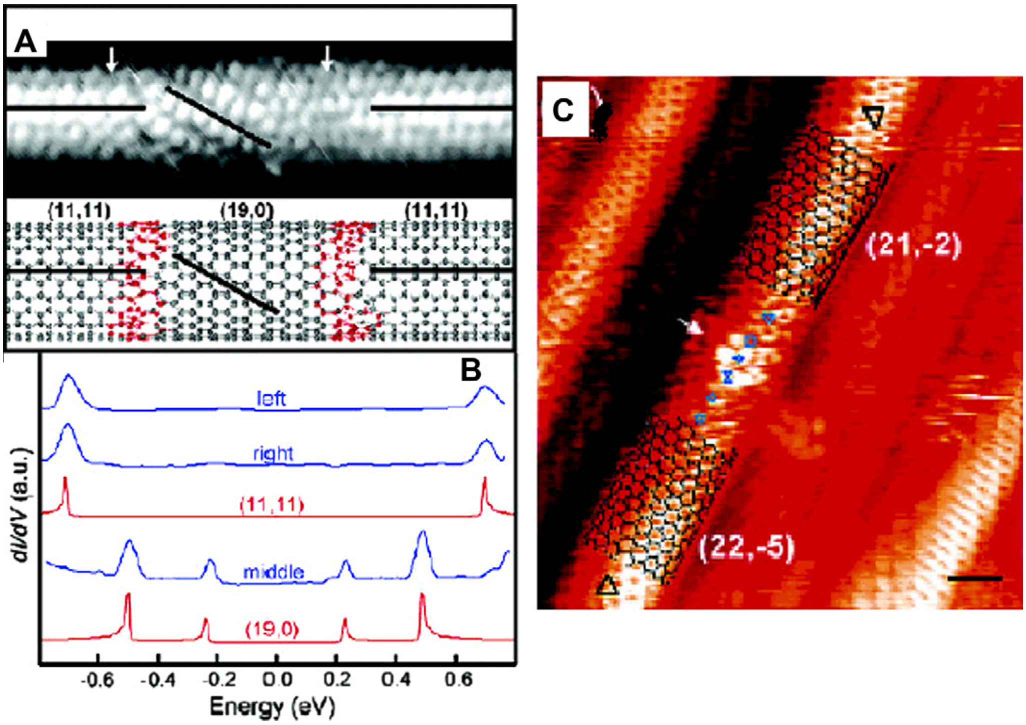

Figure 16 (A) STM atomic resolved image of Intra Molecular Junction of SWCNT. (B) STM image measurement representing the Density of States corresponding to lines in (A), (C) STM image of a SWCNT. The chirality can be determined easily.

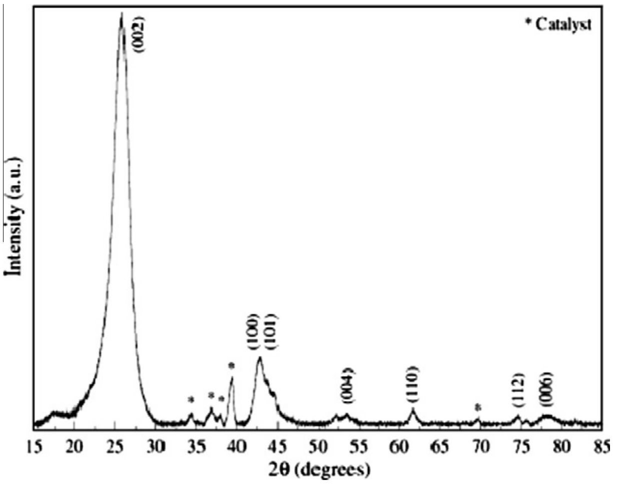

Figure 17 XRD pattern of MWCNT synthesized by CVD (diameter of about 60 nm). The incident X-ray wavelength is $\lambda = 0.154056$ nm. The most significant Bragg peaks are noticed with Miller indices. The presence of catalysts (Co and Mo) in the CNT sample is shown by stars.

Bragg law, and a family of (*hk* 0) peaks due to the honeycomb lattice of single graphene sheet. Consequently, the XRD profile is not useful to differentiate microstructural details between the CNTs and the graphite structure but can help to determinate the sample purity (Zhu et al., 2003).

X-ray diffraction show that no (0 0 2) peak can be measured with well-aligned straight CNTs on the substrate surface. In the case of CNTs with tube axis perpendicular to the substrate surface, the X-ray incident beam is scattered inside the sample and is not collected. Consequently, the intensity of the (0 0 2) peak decreases as CNTs are better aligned (Cao et al., 2001).

X-ray diffraction has also been used for studying the effect of various parameters such as the mean tube diameter, the finite size of the bundles, and the diameter dispersivity of the tubes. All these parameters affect to a significant degree the position and the width of the (1 0) peak (Rols et al., 1999; Kuzmany et al., 2001). However, this characterisation method is not a sample destructive.

7.6. Neutron diffraction

This technique is widely used for the determination of structural features such as bond length and possible distortion of hexagonal network (Burian et al., 2004). Moreover, contrary to X-ray diffraction, a wide range of scattering vector Q can be explored due to the weak decrease of the atomic factor with Q (Lambin et al., 2002). Many Bragg reflections and the use of radial distribution function allow obtaining much more structural features than X-ray.

A distinction between CNTs structural types (armchair, zigzag, and chiral) can be achieved for the smallest diameters, due to the effect of curvature and chirality on the powder diffraction pattern.

Various parameters can modify the neutron diffraction pattern such as finite size of CNT bundles, number of tubes in bundles, and CNT diameters polydispersivity (Rols et al., 1999), which allow making comparison between neutron diffraction and theoretical data (Giannasi et al., 2004).

7.7. Raman spectroscopy

Raman spectroscopy is one of the most powerful tools for characterisation of CNTs. Without sample preparation, a fast and nondestructive analysis is possible. All allotropic forms of carbon are active in Raman spectroscopy (Arepalli et al., 2004). And the position, width, and relative intensity of bands are modified according to the carbon forms (Ferrari and Robertson, 2000).

Fig. 18 summarise the most characteristic features of CNTs in Raman spectrum:

1) A_{1g} breathing mode: A low frequency peak $< 200\ \text{cm}^{-1}$ (or bunch of peaks for polydisperse samples when resonating conditions are met) characteristic of the SWCNT, whose frequency depends essentially on the diameter of the tube;
2) D line mode (disorder line): A large structure assigned to residual ill-organised graphite ($1340\ \text{cm}^{-1}$);
3) G band mode: A high frequency bunch (between 1500 and $1600\ \text{cm}^{-1}$), corresponding to a splitting of the E_{2g} stretching mode of graphite (Mamedov et al., 2002). This bunch could be superimposed with the G line of residual graphite (Hiura et al., 1993);
4) A second order observed mode between 2450 and $2650\ \text{cm}^{-1}$ assigned to the first overtone of the D mode;
5) A combination mode of the D and G modes between 2775 and $2950\ \text{cm}^{-1}$.

The active modes for a CNT are (Kuzmany et al., 1998; Bacsa et al., 2002; Damnjanovic, 1983):

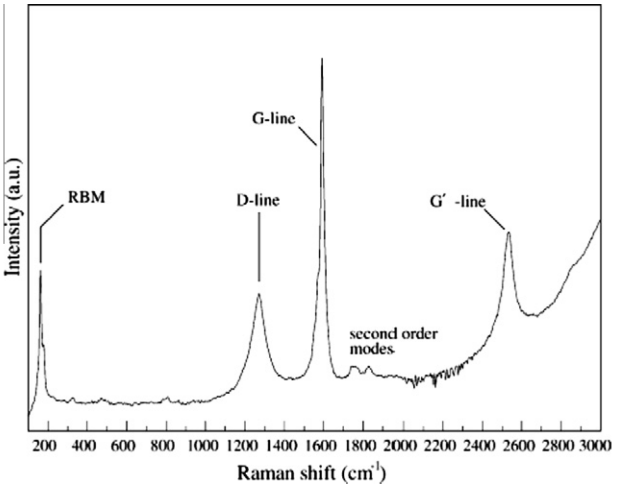

Figure 18 Raman spectrum showing the most characteristic features of CNTs produced by arc discharge method followed by air oxidation: radial breathing mode (RBM), the D band, G band and G band. Second order modes are also observed. Spectrum obtained from SWCNTs sample (diameter of about 1.07 nm) mixed with KBr using a Elaser = 1.16 eV ($\lambda = 1064.5$ nm) excitation.

$\gamma_{\mathrm{Raman}} = 2A_{1g} + 3E_{1g} + 3E_{2g}$, $\gamma_{\mathrm{IR}} = A_{2u} + 2\mathrm{E}_{1u}$ … for zigzag tubes.

$\gamma_{\mathrm{Raman}} = 2A_{1g} + 2E_{1g} + 4E_{2g}$, $\gamma_{\mathrm{IR}} = 3E_{1u}$ … for armchair tubes.

$\gamma_{\mathrm{Raman}} = 3A_1 + 5E_1 + 6E_2$, $\gamma_{\mathrm{IR}} = A_2 + 5E_1$ … for chiral tubes

Where g and u modes are Raman and IR active, respectively.

In the identification of the different tube geometries the radial breathing mode (RBM), which is a certain type of vibration, plays an important role. The RBM is directly dependent on the CNT diameters through the relation:

$$\omega_{\mathrm{RBM}} = A/d + B$$

Where: d is the CNT diameter, A and B parameters are determined experimentally (Jorio et al., 2003). However, the frequency of RBM is not related to the chiral angle θ of the CNTs (Jishi et al., 1993; Kurti et al., 1998; Sanchez-Portal et al., 1999).

Determination of the structure of a single CNT by Raman spectroscopy is possible as the density of electronic states is very large for some energy ranges in SWCNT. The density of states is an indication for the number of energy states, ΔN, per energy difference, ΔE. Every different CNT geometry, i.e., a different (n,m) pair, results in a unique pattern for the density distribution of states which can also be calculated theoretically. If the photon energy is (almost) equal to the energy needed for the valence to conduction band transition, an intense Raman signal is found as a direct result of the strong coupling between the electrons and phonons of a CNT under resonance conditions (Dresselhaus et al., 2002).

An inversely linear dependence of the RBM feature intensity on tube diameter exists if one-dimensional physical behavior is assumed (Jorio et al., 2001). After a theoretical calculation for certain geometry is performed, the RBM measured can be linked to individual CNT geometry. However, small differences in intensity and RBM frequency are caused by difference in CNT length and incompleteness of the theoretical models used. Additional differences arise for signals with almost the same RBM mode frequency if CNT chirality is different (Fig. 19).

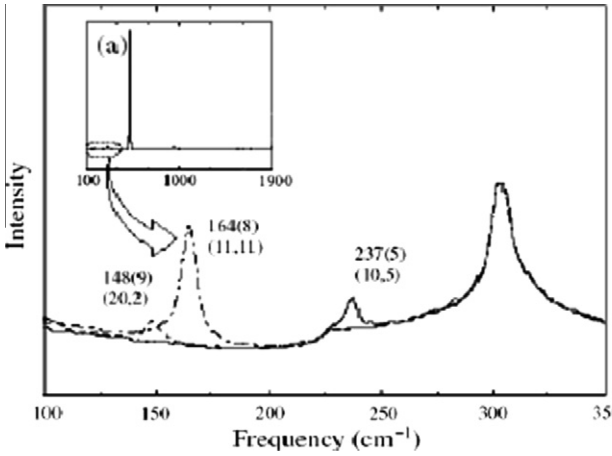

Figure 19 Raman spectra for three different spots, showing different RBMs. Each spot is clearly associated with only one RBM and thus a single nanotube. The Raman signal of the Si substrate is visible at 303 cm^{-1}.

This second way to identify the geometry of a single SWCNT enhances further fundamental research into the dependence of physical properties on CNT geometry. This is a prerequisite for detailed engineering of molecular electronics based on CNTs as CNT structure could be directly linked to physical properties for single CNTs.

The diameters and metallic/semiconducting features of SWCNTs can be characterised by studying the G band line shape although the information obtained is less accurate than that from RBM. The Raman line shape differs between metallic and semiconductor CNTs thus allowing to distinguish the two types. For semiconducting CNTs, the profile of the two components $\omega^{-}{}_{G}$ and $\omega^{+}{}_{G}$ is narrow (Colomer et al., 2001) and fits to a Lorentzian line shape (Jorio et al., 2003; Alvarez et al., 2000). However, for metallic tubes, the profile of the lower frequency component $\omega^{-}{}_{G}$ is broad, asymmetric and can be described by a Breit-Wigner-Fano (BWF) line shape Jorio et al., 2003; Colomer et al., 2001; Dresselhaus et al., 2002.

CNT have proven to be an unique system for the study of Raman spectra in one-dimensional systems (Dresselhaus et al., 2005; Jorio et al., 2004), and at the same time Raman spectroscopy has provided an exceedingly powerful tool useful in the study of the vibrational properties and electronic structures of CNT (Kavan et al., 2001; Alvarez et al., 2000), particularly for characterisation of CNT's with respect to their diameters, and quality of the samples properties (Dresselhaus et al., 2002; Astakhova et al., 2003).

Raman spectroscopy is considered an extremely powerful tool for characterising SWCNT, which gives qualitative and quantitative information on its diameter, electronic structure, purity and crystallinity, and distinguishes metallic and semiconducting, chirality (for single SWCNT). However, Local details such as size, diameter can be obtained by Raman or local electron diffraction but, to investigate CNTs at larger scale XRD or neutron diffraction is needed.

7.8. Thermal analysis (TGA/DTG)

Thermal analysis involves a dynamic phenomenological approach to the study of materials by observing the response of these materials to a change in temperature. Thermal analysis methods are useful for identifying relative changes due to processing. It is used to study the degree of CNTs purification (Arepalli et al., 2004).

Thermal gravimetric analysis (TGA) and derivative thermal gravimetric (DTG) analysis methods controlled oxidation process that gives quantitative data on the weight fractions of carbon and metal catalyst in the sample, and the temperatures of bulk oxidation events (Guggenheim and Koster van Groos, 2001) (Fig. 20).

7.9. Absorption spectroscopy (UV, Vis and IR)

Because of their unique electronic structure, CNTs and specially SWCNT have discrete optical absorptions that do not occur in other graphitic nanocarbons. Absorption spectroscopic technique is very useful as a relative purity measurement of CNT (Fig. 21).

There are 7–9 IR active modes in SWCNTs which depend on the symmetry: chiral, zigzag, and armchair (Kuhlmann

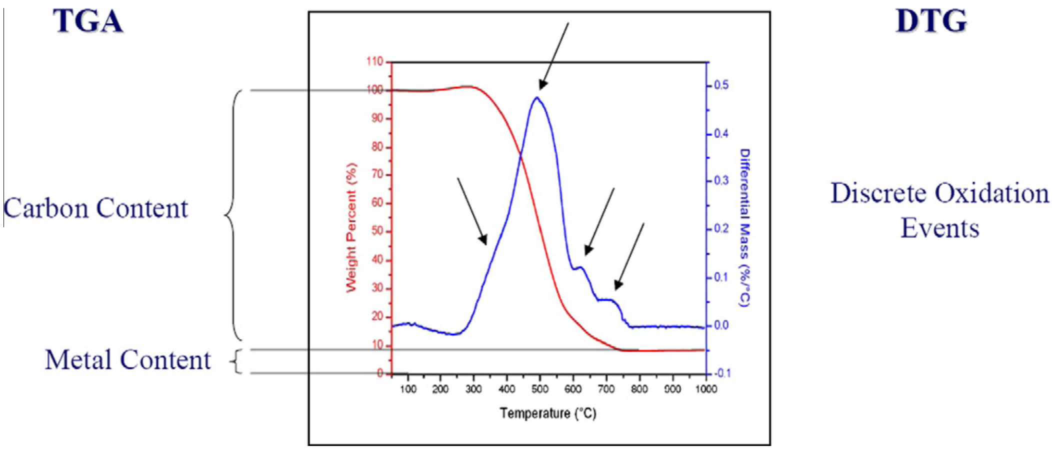

Figure 20 Analysis of CNTs by thermal methods.

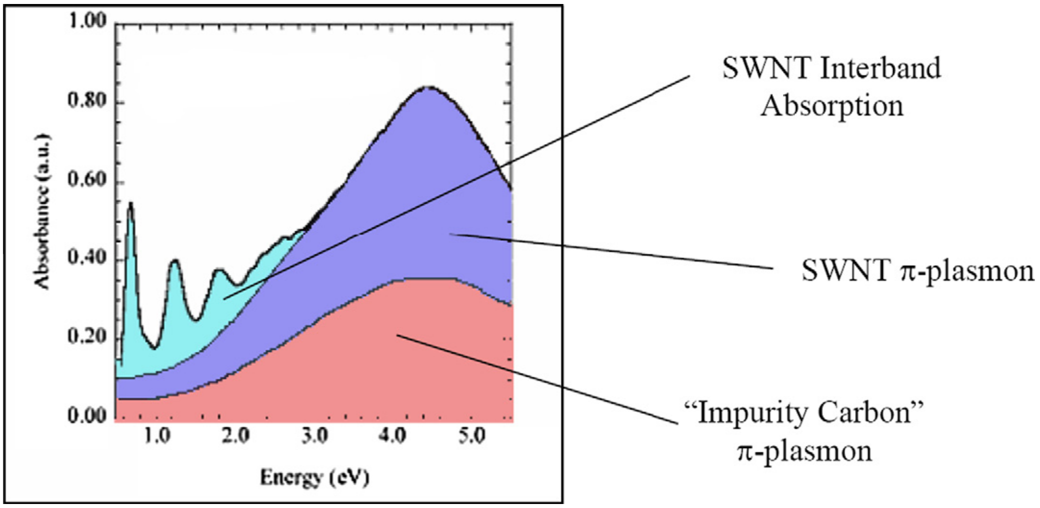

Figure 21 SWCNT Absorption spectrum (Itkis et al., 2005).

et al., 1998). The main active modes are the A_{2u} and E_{1u} modes (Kuzmany et al., 1998). With MWCNTs, these phonon modes are observed by at about 868 and 1575 cm^{-1}, respectively (Kastner et al., 1994; Eklund et al., 1995). These modes (around 850 and 1590 cm^{-1}) appear in all CNTs symmetry independently of the diameters (Kuhlmann et al., 1998). Two structures around 874 ± 2 and 1598 ± 3 cm^{-1} were shown in samples containing mostly SWCNTs. However, the frequencies deviate from the graphite frequencies to higher values by 5 and 8 cm^{-1}, respectively.

In characterisation of CNTs, IR spectroscopy is often used to determine impurities remaining from synthesis or molecules capped on the CNT surface. Numerous works are performed on organic molecules and CNTs: IR spectroscopy exhibits all the modification of the CNTs structure and reveals the nature of compounds added to the CNTs. One study characterised the reaction products of MWCNTs chemically modified by amino compounds (Saito et al., 2002). These works can be classified into two groups: characterisation of molecules attached to CNTs (He et al., 2004; Yang et al., 2004; Jung et al., 2004; Xu et al., 2003; Liu et al., 2003; Aizawa and Shaffer, 2003), catalytic properties of CNTs (Wang et al., 2004; Pereira et al., 2004).

Another study noticed the difference in catalytic activity performance between CNTs, activated carbon and graphite samples in the oxidative dehydrogenation of ethylbenzene (ODE). The highest catalytic activity is obtained with MWCNTs which are oxidised before the catalytic experiments (Pereira et al., 2004). The possibilities of the use of CNTs for catalytic removal of NO_x (NO, NO_2, NO_3) were also investigated by FT-IR (Wang et al., 2004).

Useful techniques used for CNTs. However, these characterisation methods face the following challenges:

1. No single technique can give a complete description of a CNT sample.
2. Limits to the conclusions that can be drawn from each technique.
3. Sample preparation and measurement protocol can have a big impact.
4. Measurements become more useful when compared against a reference.

5. Difficult to make direct comparisons between CNT made by different methods.

For a correct characterisation of CNTs, all these techniques described herein cannot be used separately but must be used in complementary ways.

8. Conclusion

Based on 181 references, CNTs are discussed and described in this review from their discovery to present day in terms of history, types, structure, synthesis and characterisation methods.

Nanotechnology is nowadays one of the most important trends in science, perceived as one of the key technologies of the present century. Its applications include the biotechnology and pharmacy fields as well as electronics, scientific tools, industrial manufacturing processes, and introduction of advance materials … etc. In this last aspect, nanotechnology includes the production of novel and revolutionary materials of the size of 100 nm or even smaller. CNTs are part of these novel materials.

Carbon nanotubes may have only recently caught the attention of the world but many advances have been made since their discovery. They are unique nanostructures that display the desirable properties of any other known material. The techniques of production have also come a long way but still have some efforts and time to be more efficient and cost effective.

Production methods include classical approaches such as the arc method, chemical vapour deposition, and laser ablation, new methods which are being tested such as through solar energy, plasma and microgravity environments. Production and purification methods change types, yields, and structural surfaces of CNTs. As a result, there may be change in the electrical and mechanical properties, and actual structure of CNTs. Therefore, the main thrust of the research should be in the area of producing and purifying CNTs in a single and efficient step process to conserve the fascinating features of CNTs.

Although there are not so many techniques available for CNTs characterisation, Useful techniques for CNTs characterisation are used. X-ray photoelectron spectroscopy allows determining the functionalisation of the CNTs. Scanning tunneling microscopy is a powerful technique used to obtain three-dimensional images and electronic states of the CNTs. X-ray diffraction is used to obtain some information on the interlayer spacing, the structural strain and the impurities. Numerous features such as intershell spacing, chiral indices, and helicity are also obtained by transmission electron microscopy. Infrared spectroscopy is often used to determine impurities remaining from synthesis or molecules capped on the CNT surface. But the most powerful technique to characterise CNTs remains the Raman spectroscopy: without sample preparation, a fast and nondestructive analysis is possible. Moreover, Raman spectra simulations are performed on various CNTs geometries.

Carbon nanotubes are an example of true nanotechnology: only a nanometer in diameter, but molecules that can be manipulated chemically and physically. CNTs have amazing and unique electronic, physical, chemical, and mechanical properties, which lead to incredible forms of strength, and conductivity. They open incredible and endless applications in materials, electronics, chemical processing and energy management, as it will be seen in the next part.

References

Agrawal, B.K., Agrawal, S., Srivastava, R., 2004. J. Phys. Condens. Matter 16, 1467.

Aizawa, M., Shaffer, M., 2003. Chem. Phys. Lett. 368, 121.

Alford, J.M., Mason, G.R., Feikema, D.A., 2001. Sixth international microgravity combustion workshop, NASA Glenn Research Center, Cleveland, OH, CP-2001-210826, p. 293, May 22–24.

Alvarez, L., Righi, A., Guillard, T., Rols, S., Anglaret, E., Laplaze, D., Sauvajol, J.-L., 2000. Chem. Phys. Lett. 316, 186.

Arepalli, S., Nikolaev, P., Gorelik, O., Hadjiev, V., Holmes, W., Files, B., Yowell, L., 2004. Carbon 42, 1783.

Arepalli, S., Nikolaev, P., Gorelik, O., Hadjiev, V.G., Holmes, W., Files, B., Yowell, L., 2004. Carbon 42, 1783.

Astakhova, T. Yu., Vinogradov, G.A., Menon, M., 2003. Russ. Chem. Bull., Int. Ed. 52 (4), 823.

Ayumu, Y., Noboru, K., Wataru, M., 2002. J. Phys. Chem. B 106 (51), 13294.

Bacsa, R.R., Peigney, A., Laurent, C., Puech, P., Bacsa, W.S., 2002. Phys. Rev. B 65, 161404.

Bandow, S., Rao, A.M., Williams, K.A., Thess, A., Smalley, R.E., Eklund, P.C., 1997. J. Phys. Chem. B 101, 44.

Barkauskas, J., Stankevičiene, I., Selskis, A., 2010. Sep. Purif. Technol. 71, 331.

Bolshakov, A.P., Uglov, S.A., Saveliev, A.V., Konov, V.I., Gorbunov, A.A., Pompe, W., Graff, A., 2002. Diam. Relat. Mater. 11, 3.

Borowiak-Palen, E., Pichler, T., Liu, X., Knupfer, M., Graff, A., Jost, O., Pompe, W., Kalenczuk, R.J., Fink, J., 2002. Chem. Phys. Lett. 363, 567.

Bronikowski, M.J., Willis, P.A., Colbert, D.T., Smith, K.A., Smalley, R.E., 2001. J. Vac. Sci. Technol. A – Vac. Surf. Films 19, 1800.

Burian, A., Koloczk, J., Dore, J., Hannon, A.C., Nagy, J.B., Fonseca, A., 2004. Diam. Relat. Mater. 13, 1261.

Cao, A., Xu, C., Liang, J., Wu, D., Wei, B., 2001. Chem. Phys. Lett. 344, 13.

Charlier, A., McRae, E., Heyd, R., Charlier, M., Moretti, D., 1999. Carbon 37, 1779.

Chen, P., Wu, X., Sun, X., Lin, J., Ji, W., Tan, K., 1999. Phys. Rev. Lett. 82, 2548.

Chen, Y., Liu, C., Li, F., Cheng, H.M., 2006. J. Porous Mater. 13, 141.

Chiang, I.W., Brinson, B.E., Smalley, R.E., Margrave, J.L., Hauge, R.H., 2001. J. Phys. Chem. B 105 (6), 1157.

Chiang, I.W., Brinson, B.E., Huang, A.Y., Willis, P.A., Bronikowski, M.J., Margrave, J.L., Smalley, R.E., Hauge, R.H., 2001. J. Phys. Chem. B 105 (35), 8297.

Clauss, W., Bergeron, D., Johnson, A., 1998. Phys. Rev. B 58, R4266.

Collins, P.G., Avouris, P., 2000. Nanotubes for Electronics – Scientific American, page 67, December 2000.

Colomer, J., Benoit, J., Stephan, C., Lefrant, S., Van Tendeloo, G., Nagy, J.B., 2001. Chem. Phys. Lett. 345, 11.

Daenen, M., de Fouw, R.D., Hamers, B., Janssen, P.G.A., Schouteden, K., Veld, M.A.J., 2003. The Wondrous World of Carbon Nanotubes, a review of current carbon nanotube technologies, Eindhoven University of Technology, February 2003.

Dai, H., 2002. Surf. Sci. 500, 218.

Damnjanovic, M., 1983. Phys. Lett. A 94, 337.

Dolmer, S., 20003. http://www.inano.dk/sw180.asp. Denmark. [online] available.

Dresselhaus, M.S., Dresselhaus, G., Saito, R., 1995. Carbon 33, 883.

Dresselhaus, M., Dresselhaus, G., Saito, R., 1995. Carbon 33, 883.

Dresselhaus, M.S., Dresselhaus, G., Eklund, P.C., 1996. Science of Fullerenes and Carbon Nanotubes. Academic Press, New York, USA.

Dresselhaus, M.S., Dresselhaus, G., Jorio, A., Souza Filho, A.G., Pimenta, M.A., Saito, R., 2002. Acc. Chem. Res. 35, 1070.

Dresselhaus, M., Dresselhaus, G., Jorio, A., Souza-Filho, A.G., Saito, R., 2002. Carbon 40, 2043.

Dresselhaus, M.S., Dresselhaus, G., Saito, R., Jorio, A., 2005. Phys. Rep. 409, 47.

Droppa, R., Hammer, P., Carvalho, A., Dos Santos, M., Alvarez, F., 2002. J. Non-Cryst. Solids 299–302, 874.

Duan, H.M., McKinnon, J.T., 1994. J. Phys. Chem. 98 (49), 12815.

Ebbesen, T.W. (Ed.), 1997. Carbon Nanotubes: Preparation and properties, CRC Press, Boca Raton, Fla USA, p. 139.

Ebbesen, T.W., Ajayan, P.M., 1992. Nature 358, 220.

Eklund, P., Holden, J., Jishi, R., 1995. Carbon 33, 959.

Eklund, P.C., Pradhan, B.K., Kim, U.J., Xiong, Q., Fischer, J.E., Friedman, A.D., Holloway, B.C., Jordan, K., Smith, M.W., 2002. Nano Lett. 2, 6.

Farkas, E., Anderson, M.E., Chen, Z.H., Rinzler, A.G., 2002. Chem. Phys. Lett. 363, 111.

Ferrari, A., Robertson, J., 2000. Phys. Rev. B 61, 14095.

Flahaut, E., Bacsa, R., Peigney, A., Laurent, C., 2003. Chem. Commun. 12, 1442.

Gao, B., Bower, C., Lorentzen, J.D., Fleming, L., Kleinhammes, A., Tang, X.P., Mcneil, L.E., Wu, Y., Zhou, O., 2000. Chem. Phys. Lett. 327, 69.

Georgakilas, V., Voulgaris, D., Vázquez, E., Prato, M., Guldi, M.D., Kukovecz, A., Kuzmany, H., 2002. J. Am. Chem. Soc. 124 (48), 14318.

Giannasi, A., Celli, M., Sauvajol, J., Zoppi, M., Bowron, D., 2004. Physica B 350, e1027.

Gommes, C., Blacher, S., Masenelli-Varlot, K., Bossuot, C., McRae, E., Fonseca, A., Nagy, J.B., Pirard, J.P., 2003. Carbon 41, 2561.

Gu, Z., Peng, H., Hauge, R.H., Smalley, R.E., Margrave, J.L., 2002. Nano Lett. 2 (9), 1009.

Guggenheim, S., Koster van Groos, A.F., 2001. Clays Clay Miner. 49 (5), 433.

Guo, T., Nikolaev, P., Thess, A., Colbert, D.T., Smalley, R.E., 1995. Chem. Phys. Lett. 243, 49.

Guo, T., Nikolaev, P., Rinzler, A.G., Tomhek, D., Colbert, D.T., Smalley, R.E., 1995. J. Phys. Chem. 99, 10694.

Guo, J., Yang, C., Li, Z.M., Bai, M., Liu, H.J., Li, G.D., Wang, E.G., Chan, C.T., Tang, Z.K., Ge, W.K., Xiao, X., 2004. Phys. Rev. Lett. 93, 017402.

Hafner, J.H., Bronikowski, M.J., Azamian, B.R., Nikolaev, P., Rinzler, A.G., Colbert, D.T., Smith, A., Smalley, R.E., 1998. Chem. Phys. Lett. 296, 195.

Hajime, G., Terumi, F., Yoshiya, F., Toshiyuki, O., 2002. Method of purifying single wall carbon nanotubes from metal catalyst impurities. Honda Giken Kogyo Kabushiki Kaisha, Japan.

Hamada, N., Sawada, S., Oshiyama, A., 1992. Phys. Rev. Lett. 68, 1579.

Hammer, P., Victoria, N., Alvarez, F., 2000. J. Vac. Sci. Technol. 18, 2277.

Harris, P., 2003. A Carbon Nanotube Page, Chemistry Department of the University of Reading, http://www.personal.rdg.ac.uk/˜scsharip/tubes.htm. [online] Available.

Harutyunyan, A.R., Pradhan, B.K., Chang, J.P., Chen, G.G., Eklund, P.C., 2002. J. Phys. Chem. B 106 (34), 8671.

Hassanien, A., Tokumoto, M., 2004. Carbon 42, 2649.

He, B., Sun, W., Wang, M., Liu, S., Shen, Z., 2004. Mater. Chem. Phys. 84, 140.

Hiura, H., Ebbesen, T., Tanigaki, K., Takahashi, H., 1993. Chem. Phys. Lett. 202, 509.

Houjin, H., Masashi, S., Atsuo, Y., Hisashi, K., Masafumi, A., 2001. JP10713, p. 0245812.

Hsu, T.R., 2002. MEMS and Microsystems: Design and Manufacture. McGraw-Hill, Boston, MA.

Hsu, W.K., Hare, J.P., Terrones, M., Kroto, H.W., Walton, D.R.M., Harris, P.J.F., 1995. Nature 377, 687.

Hu, H., Bhowmik, P., Zhao, B., Hamon, M.A., Itkis, M.E., Haddon, R.C., 2001. Chem. Phys. Lett. 345, 25.

Huang, S.M., Dai, L.M., 2002. J. Phys. Chem. B 106 (14), 3543.

Ichimura, K., Osawa, M., Nomura, K., Kataura, H., Maniwa, Y., Suziki, S., Achiba, Y., 2002. Phys. B: Condens. Matter 323, 230.

Iijima, S., 1991. Nature (London) 354, 56.

Iijima, S., 1998. Micro Electro Mechanical Systems. IEEE, Heidelberg, Germany, p. 520.

Iijima, S., Ichihashi, T., 1993. Nature (London) 363, 603.

Itkis, M.E., Perea, D.E., Jung, R., Niyogi, S., Haddon, R.C., 2005. J. Am. Chem. Soc. 127, 3439.

Jishi, R., Venkataraman, L., Dresselhaus, M., Dresselhaus, G., 1993. Chem. Phys. Lett. 209, 77.

Jorio, A., Saito, R., Hafner, J.H., Lieber, C.M., Hunter, M., McClure, T., Dresselhaus, G., Dresselhaus, M.S., 2001. Phys. Rev. Lett. 86, 1118.

Jorio, A., Pimenta, M., Souza-Filho, A., Saito, R., Dresselhaus, G., Dresselhaus, M., 2003. New J. Phys. 5, 139.1.

Jorio, A., Pimenta, M.A., Fantini, C., Souza, M., Souza Filho, A.G., Samsonidze, G.G., Dresselhaus, G., Dresselhaus, M.S., Saito, R., 2004. Carbon 42, 1067.

Jose-Yacaman, M., Miki-Yoshida, M., Rendou, L., Santiesteban, J.S., 1993. Appl. Phys. Lett. 62, 657.

Journet, C., Bernier, P., 1998. Appl. Phys. A 67, 1.

Journet, C., Bernier, P., 1998. Appl. Phys. A-Mater. Sci. Process. 67 (1), 1.

Jung, S.H., Kim, M.R., Jeong, S.H., Kim, S.U., Lee, O.J., Lee, K.H., Suh, J.H., Park, C.K., 2003. Appl. Phys. A-Mater. Sci. Process. 76 (2), 285.

Jung, D., Ko, Y.K., Jung, H., 2004. Mater. Sci. Eng. C 24, 117.

Kajiura, H., Tsutsui, S., Huang, H.J., Murakami, Y., 2002. Chem. Phys. Lett. 364, 586.

Kastner, J., Pichler, T., Kuzmany, H., Curran, S., Blau, W., Weldon, D.N., Delamesiere, M., Draper, S., Zandbergen, H., 1994. Chem. Phys. Lett. 221, 53.

Kavan, L., Rapta, P., Dunsch, L., Bronikowski, M.J., Willis, P., Smalley, R.E., 2001. J. Phys. Chem. B 105, 10764.

Kiang, C., Endo, M., Ajayan, P., Dresselhaus, G., Dresselhaus, M., 1998. Phys. Rev. Lett. 81, 1869.

Kim, P., Odom, T., Huang, J., Lieber, C., 2000. Carbon 38, 1741.

Kingston, C., 2007. Challenges in the Characterization of Carbon Nanotubes: the Need for Standards, Molecular and Nanomaterial Architectures Group Tri-National Workshop on Standards for Nanotechnology, February 2007.

Kingston, T.C., Jakubek, Z.J., Dénommée, S., Simard, B., 2004. Carbon 42, 1657.

Krasheninnikov, A., 2001. Solid State Commun. 118, 361.

Kroto, H.W., Heath, J.R., O'Brien, S.C., Curl, R.F., Smalley, R.E., 1985. Nature 318, 162.

Kuhlmann, U., Jantoljak, H., Pfander, M., Bernier, P., Journet, C., Thomsen, C., 1998. Chem. Phys. Lett. 294, 237.

Kurti, J., Kresse, G., Kuzmany, H., 1998. Phys. Rev. B 58, R8869.

Kuzmany, H., Burger, B., Thess, A., Smalley, R., 1998. Carbon 36, 709.

Kuzmany, H., Plank, W., Hulman, M., Kramberger, Ch., Gruneis, A., Pichler, Th., Peterlik, H., Kataura, H., Achiba, Y., 2001. Eur. Phys. J. B 22, 307.

Lambin, P., Loiseau, A., Culot, C., Biro, L., 2002. Carbon 40, 1635.

Laplaze, D., Bernier, P., Maser, W.K., Flamant, G., Guillard, T., Loiseau, A., 1998. Carbon 36, 685.

Lauret, J.S., Voisin, C., Cassabois, G., Roussignol, P., Delalande, C., Filoramo, A., Capes, L., Valentin, E., Jost, O., 2004. Physica E 21, 1057.

Lebedkin, S., Hennrich, F., Skipa, T., Kappes, M.M., 2003. J. Phys. Chem. B 107, 1949.

Lee, Y., Cho, T., Lee, B., Rho, J., An, K., Lee, Y., 2003. J. Fluorine Chem. 120, 99.

Lee, S.M., Lee, S.C., Jung, J.H., Kim, H.J., 2005. Chem. Phys. Lett. 416, 251.

Lefebvre, J., Fraser, J.M., Homma, Y., Finnie, P., 2004. Appl. Phys. A78, 1107.

Li, W.Z., 2003. Chin. Phys. Lett. 368, 299.

Liang, W.Z., Chen, G.H., Li, Z., Tang, Z.K., 2002. Appl. Phys. Lett. 80, 3415.

Liming, Y., Saito, K., Pan, C., Williams, F.A., Gordon, A.S., 2001a. Chem. Phys. Lett. 340, 237.

Liming, Y., Saito, K., Hu, W., Chen, Z., 2001b. Chem. Phys. Lett. 346, 23.

Lin, N., Ding, J., Yang, S., Cue, N., 1996. Carbon 34, 1295.

Liu, J., Harris, A.T., 2008. Sep. Purif. Technol. 62, 602.

Liu, X., Pichler, T., Knupfer, M., Golden, M.S., Fink, J., Kataura, H., Achiba, Y., 2002. Phys. Rev. B 66, 045411.

Liu, L., Qin, Y., Guo, Z., Zhu, D., 2003. Carbon 41, 331.

Liu, Y., Shen, Z., Yokogawa, K., 2006. Mater. Res. Bull. 41, 1503.

Liu, J., Dunens, O.M., Mackenzie, K.J., See, C.H., Harris, A.T., 2008. AIChE J. 54, 3303.

Machon, M., Reich, S., Thomsen, C., Sanchez-Portal, D., Ordejon, P., 2002. Phys. Rev. B 66, 155410.

MacKenzie, K., Dunens, O., Harris, A.T., 2009. Sep. Purif. Technol. 66, 209.

Mamedov, A.A., Kotov, N.A., Prato, M., Guldi, D.M., Wicksted, J.P., Hirsch, A., 2002. Nat. Mater. 1, 190.

Masako, Y., Rie, K., Takeo, M., Yoshimasa, O., Susumu, Y., Etsuro, O., 1995. Appl. Phys. Lett. 67, 17.

Masako, Y., Rie, K., Yoshimasa, O., Etsuro, O., Susumu, Y., 1997. Appl. Phys. Lett. 70, 14.

Maser, W.K., Munoz, E., Benito, A.M., Martinez, M.T., de la Fuente, G.F., Maniette, Y., Anglaret, E., Sauvajol, J.L., 1998. Chem. Phys. Lett. 292, 587.

Mawhinney, D.B., Naumenko, V., Kuznetsova, A., Yates Jr., J.T., Liu, J., Smalley, R.E., 2000. Chem. Phys. Lett. 324, 213.

Mintmire, J., Dunlap, B., White, C., 1992. Phys. Rev. Lett. 68, 631.

Miyauchi, Y., Chiashi, S., Murakami, Y., Hayashida, Y., Maruyama, S., 2004. Chem. Phys. Lett. 387, 198.

Moon, J.M., An, K.H., Lee, Y.H., Park, Y.S., Bae, D.J., Park, G.S., 2001. J. Phys. Chem. B 105 (24), 5677.

Morinobu, E., Kenji, T., Susumu, I., Kiyoharu, K., Minoru, S., Harold, K.W., 1993. J. Phys. Chem. Solids 54, 12.

Murakami, Y., Miyauchi, Y., Chiashi, S., Maruyama, S., 2003. Chem. Phys. Lett. 377, 49.

Murr, L.E., Bang, J.J., Esquivel, E.V., Guerrero, P.A., Lopez, D.A., 2004. J. Nanoparticle Res. 6, 241.

Nikolaev, P., Bronikowski, M.J., Bradley, R.K., Rohmund, F., Colbert, D.T., Smith, K.A., Smalley, R.E., 1999. Chem. Phys. Lett. 313, 91.

Niu, J.J., Wang, J.N., Jiang, Y., Su, L.F., Ma, J., 2007. Microporous Mesoporous Mater. 100, 1.

Niyogi, S., Hu, H., Hamon, M.A., Bhowmik, P., Zhao, B., Rozenzhak, S.M., Chen, J., Itkis, M.E., Meier, M.S., Haddon, R.C., 2001. J. Am. Chem. Soc. 123 (4), 733.

Nordström, M., Nyrup, S., 2004. Physics Institute at the Technical University of Denmark with help of Jakob Svagin, August 2004.

Obraztsova, E., Yurov, V., Shevluga, V., Baranovsky, R., Nalimova, V., Kuznetsov, V., Zaikovskii, V., 1999. Nanostruct. Mater. 11, 295.

O'Connell, M.J., Bachilo, S.M., Huffman, C.B., Moore, V.C., Strano, M.S., Haroz, E.H., Rialon, K.L., Boul, P.J., Noon, W.H., Kittrell, C., Ma, J., Hauge, R.H., Weisman, R.B., Smalley, R.E., 2003. Science 297, 503.

Odom, T., Huang, J., Kim, P., Lieber, C., 1998. Nature 391, 62.

Ouyang, M., Huang, J.L., Cheung, C.L., Lieber, C.M., 2001. Science 292, 702.

Ouyang, M., Huang, J.L., Lieber, C.M., 2002. Acc. Chem. Res. 35 (12), 1018.

Paradise, M., Goswami, T., 2007. Mater. Des. 28, 1477.

Peigney, A., Laurent, C., Flahaut, E., Bacsa, R., Rousset, A., 2001. Carbon 39, 507.

Pereira, M., Figueiredo, J., Orfao, J., Serp, P., Kalck, P., Kihn, Y., 2004. Carbon 42, 2807.

Pham-Huu, C., Keller, N., Roddatis, V., Mestl, G., Schlogl, R., Ledoux, M.J., 2002. Phys. Chem. Chem. Phys. 4, 514.

Qin, L.C., Zhao, X., Hirahara, K., Miyamoto, Y., Ando, Y., Iijima, S., 2000. Nature 298, 50.

Ren, Z.F., Huang, Z.P., Xu, J.W., Wang, J.H., Bush, P., Siegal, M.P., Provencio, P.N., 1998. Science 282, 1105.

Ren, Z.F., Huang, Z.P., Xu, J.W., Wang, J.H., Bush, P., Siegel, M.P., Provencio, P.N., 1998. Science (Washington, DC) 282, 5391.

Ren, Z.F., Huang, Z.P., Xu, J.W., Wang, H.J., Bush, P., Siegal, M.P., Provencio, P.N., 1998. Science 282, 1105.

Ren, Z.F., Huang, Z.P., Wang, D.Z., Wen, J.G., Xu, J.W., Wang, J.H., Calvet, L.E., Chen, J., Klemic, J.F., Reed, M.A., 1999. Appl. Phys. Lett. 75, 8.

Roco, M.C., 1999. Nanotechnology Brochure, Shaping the World Atom by Atom, National Science and Technology Council (NSTC), Committee on Technology, the Interagency Working Group on Nanoscience, Engineering and Technology (IWGN), September 1999.

Rols, S., Almairac, R., Henrard, L., Anglaret, E., Sauvajol, J., 1999. Eur. Phys. J. B 10, 263.

Safarova, K., Dvorak, A., Kubinek, R., Vujtek, M., Rek, A., 2007. Modern Research and Educational Topics in Microscopy, FORMATEX 2007.

Saito, R., Fujita, M., Dresselhaus, G., Dresselhaus, M., 1992. Appl. Phys. Lett. 60, 2204.

Saito, Y., Okuda, M., Tomita, M., Hayashi, T., 1995. Chem. Phys. Lett. 236, 419.

Saito, R., Dresselhaus, G., Dresselhaus, M., 2000. Phys. Rev. B 6, 2981.

Saito, R., Matsushige, K., Tanaka, K., 2002. Phys. B: Condens. Matter 323, 280.

Sanchez-Portal, D., Artacho, E., Soler, J., Rubio, A., Ordejon, P., 1999. Phys. Rev. B 59, 12768.

Sano, N., Chhowalla, M., Roy, D., Amaratunga, G.A.J., 2002. Phys. Rev. B 66, 113403.

Sattler, K., 1995. Carbon 33, 915.

Scott, C.D., Arepalli, S., Nikolaev, P., Smalley, R.E., 2001. Appl. Phys. A: Mater. Sci. Process. 72, 5.

See, C.H., Harris, A.T., 2007. Ind. Eng. Chem. Res. 46 (4), 997.

Shelimov, K.B., Esenaliev, R.O., Rinzler, A.G., Huffman, C.B., Smalley, R.E., 1998. Chem. Phys. Lett. 282, 429.

Singer, J.M., Grumer, J., 1959. Proc. Combust. Inst. 7, 559.

Sinnot, S.B., Andrews, R., Qian, D., Rao, A.M., Mao, Z., Dickey, E.C., Derbyshire, F., 1999. Chem. Phys. Lett. 315, 25.

Suzuki, S., Watanabe, Y., Ogino, T., Heun, S., Gregoratti, L., Barinov, A., Kaulich, B., Kiskinova, M., Zhu, W., Bower, C., Zhou, O., 2002. Phys. Rev. B 66, 035414.

Tanaka, K., Yamabe, T., Fukui, K., 1999. The Science and Technology of Carbon Nanotubes, First ed. Elsevier, Oxford.

Tang, Z.K., Wang, N., Zhang, X.X., Wang, J.N., Chan, C.T., Sheng, P., 2003. New J. Phys. 5, 146.1.

Tang, Z.K., Zhang, L.Y., Wang, N., Zhang, X.X., Wang, J.N., Li, G.D., Li, Z.M., Wen, G.H., Chan, C.T., Sheng, P., 2003. Synth. Met. 133–134, 689.

Thess, A., Lee, R., Nikolaev, P., Dai, H., Petit, P., Robert, J., Xu, C., Lee, Y.H., Kim, S.G., Rinzler, A.G., Colbert, D.T., Scuseria, G.E., Tománek, D., Fischer, J.E., Smalley, R.E., 1996. Science 273 (5274), 483.

Thien-Nga, L., Hernadi, K., Ljubovic, E., Garaj, S., Forro, L., 2002. Nano Lett. 2 (12), 1349.

Thostenson, E., Ren, Z., Chou, T., 2001. Comput. Sci. Technol. 61, 1899.

Vander, W., Randall, L., Thomas, M.T., 2001. J. Phys. Chem. B 105, 42.

Wal, R.L.V., Berger, G.M., Hall, L.J., 2002. J. Phys. Chem. B 106 (14), 3564.

Wang, S., Zhu, W., Liao, D., Ng, C., Au, C., 2004. Catal. Today 93–95, 711.

Weisman, R.B., Bachilo, S.M., Tsyboulski, D., 2004. Appl. Phys. A 78, 1111.

Wildoer, J., Venema, L., Rinzler, A., Smalley, R., Dekker, C., 1998. Nature 391, 59.

Xiang, H.P., Liu, C., Tong, Y., Liu, M., Cheng, H.M., 2001. J. Mater. Res. 16 (9), 2526.

Xu, M., Huang, Q., Chen, Q., Guo, P., Sun, Z., 2003. Chem. Phys. Lett. 375, 598.

Yang, Z., Chen, H., Cao, L., Li, H., Wang, M., 2004. Mater. Sci. Eng. B 106, 73.

Yildirim, T., Gülseren, O., Kılıç, Ç., Ciraci, S., 2000. Phys. Rev. B 62, 19.

Yudasaka, M., Yamada, R., Sensui, N., Wilkins, T., Ichihashi, T., Iijima, S., 1999. J. Phys. Chem. B 103, 30.

Zhao, B., Hu, H., Niyogi, S., Itkis, M.E., Hamon, M.A., Bhowmik, P., Meier, M.S., Haddon, R.C., 2001. J. Am. Chem. Soc. 123 (47), 11673.

Zhao, X., Liu, Y., Inoue, S., Suzuki, T., Jones, R.O., Ando, Y., 2004. Phys. Rev. Lett. 92, 125502.

Zhu, W., Miser, D., Chan, W., Hajaligol, M., 2003. Mater. Chem. Phys. 82, 638.